

Development and Evaluation of a Torque-Vectoring Algorithm on RWD Racing Cars using a Dual Clutch

Mia Grahovic
Madeleine Rosicki



LUND
UNIVERSITY

Department of Automatic Control

MSc Thesis
TFRT- 6081
ISSN 0280-5316

Department of Automatic Control
Lund University
Box 118
SE-221 00 LUND
Sweden

© 2019 by Mia Grahovic & Madeleine Rosicki. All rights reserved.
Printed in Sweden by Tryckeriet i E-huset
Lund 2019

Abstract

Vehicle safety and vehicle performance are becoming more and more important for the society and many students, doctoral students, and researchers are interested in this field. Formula Student is a student competition that enables students to develop their own racing vehicles without any strict rules on how the vehicle should be controlled. The competition rules are instead directed into vehicle design and maneuverability on the track. This thesis was performed in collaboration with Lund Formula Student and BorgWarner. It presents a torque-vectoring algorithm that is planned to be implemented on a Formula Student car for next years competition in 2021. The Formula Student car will use a double clutch that is also developed at BorgWarner by a student in Mechanical Engineering at Lund University. The double clutch enables independent control of torques for each rear wheel.

The algorithm was developed in MATLAB/Simulink, mainly using vehicle models provided by BorgWarner. The goal with the torque-vectoring algorithm is to improve the vehicle's accelerating behavior while cornering.

The nonlinear model that uses a torque-vectoring dual clutch (TVDC) is compared to another nonlinear vehicle model that represents a Formula Student vehicle using a limited slip differential (LSD) clutch. The controller is using yaw rate as a control signal. The results show that the vehicle trajectories for a lane change and U-turn coincide with the reference value, for the circular path, whereas the actual yaw rate value diverges from the reference value after some time. Overall, the vehicle can better follow the desired path with the proposed torque-vectoring algorithm for a double clutch than a vehicle using an LSD clutch. When the vehicle is accelerating, it is clearly seen that for the TVDC, the actual yaw rate is following the desired yaw rate better than using open differential (OD) or LSD. Considering the yaw-rate error analysis, it is clearly seen that the error is smaller for a lane change and a U-turn than it is when the vehicle is following a circular path. Overall, the yaw-rate error is smaller when employing TVDC than without.

Acknowledgments

We would like to thank a lot of people that in one way or another contributed with their technical expertise, solutions, support, and valuable opinions throughout this thesis.

Firstly, we wish to thank our main supervisor at BorgWarner, Mariann Kempe, for your help and feedback along the way. We are thankful for having introduced us to other employees at BorgWarner, who in turn have given us valuable opinions and inputs. When problem arose along the way, we were quickly given supplies and suggestions on alternatives approaches to how to improve the control algorithm. We are especially thankful for giving us the opportunity to visit Ljungbyhed Park to try out cars implemented with different algorithms by BorgWarner's employees.

We particularly want to thank our former advisor, Ted Brink at BorgWarner, who introduced us to this project and made sure we were given all the help and resources needed.

Secondly, we would also like to express our appreciation to Pierre Petersson, an employee at BorgWarner, who suggested a vehicle model. We are thankful to him for providing great technical insight into how to make improvements in the project, and to his expertise concerning torque vectoring. Advice given from Pierre has been a great help in understanding vehicle dynamics and torque vectoring in general.

Special thanks to Jonas Dürango, consultant at BorgWarner, for gladly helping us out with the software implementation in MATLAB/Simulink. His willingness to give his time so generously and his help has been most appreciated.

Our supervisor from Lund University, Dr. Björn Olofsson, has been supportive and contributing with excellent ideas on automatic control as well as great feedback on our project during this entire semester.

Another thank you to Olofsson and Kempe for their time to read this report and providing suggestions on improvements of our thesis.

We are also grateful to our examiner, Prof. Rolf Johansson, for contributing with valuable and constructive feedback on our thesis.

We wish to thank students from the Lund Formula project team at Lund University for taking their time to answer all of our questions, providing us with good discussions, and for their assistance with the collection of the data needed.

We also would like to thank all the other employees we had the privilege to meet at BorgWarner, who were involved or showed interest in our project and contributed with valuable opinions throughout this thesis.

Work ethic and assistance provided between us has been highly appreciated.

Finally, I (Madeleine) would like to thank my father for his neverending and inestimable love and support but also his encouragement throughout my entire study.

I (Mia) want to show my great gratitude towards my parents for their support during my study at Lund University.

To each and every one of you, thank you!

Contents

List of Figures	7
List of Tables	8
1. Introduction	12
1.1 Background	13
1.2 Previous Work on Torque Vectoring	14
1.3 Purpose and Goals	15
1.4 Contribution	16
1.5 Delimitations and Assumptions	16
1.6 Challenges	17
1.7 Thesis Outline	17
2. Vehicle Dynamics	19
2.1 Vehicle Axis System	19
2.2 The Tire Behavior	20
2.3 The Single Track Model	22
2.4 Under-Steer Gradient	24
2.5 Global Coordinates	25
3. Torque Vectoring	26
3.1 Yaw Stability Control	29
4. Model Parameters and Sensor Signals	31
4.1 Data Collection	31
4.2 Vehicle Model Parameters	33
5. Control Strategy	35
5.1 Vehicle Performance Criteria	35
5.2 Modeling	35
5.3 Different Modeling Strategies	36
5.4 Control Algorithm	39
5.5 Controller Implementation Aspects	43
6. The PI Controller Tuning Process	45
6.1 PI Controller for the Nonlinear Model	45

Contents

7. Simulation Results	47
7.1 Linear Model	47
7.2 Nonlinear Model	51
7.3 Yaw-Rate Error Analysis	59
8. Discussion and Conclusions	63
Bibliography	65

List of Figures

2.1	The vehicle axis system.	20
2.2	Lateral tire slip angle of the front wheel.	21
2.3	The single track model.	22
3.1	The maximum tire friction circle without torque vectoring [12].	27
3.2	The maximum tire friction circle with torque vectoring [12].	28
4.1	Maximum combustion-engine torque on the crankshaft.	32
5.1	Block diagram of the linear model with PI controller for different velocities. In this figure, the longitudinal velocity is set to 5 m/s, the steering wheel angle is set to $\pi/2$ rad, and the desired yaw rate is set to 0.3 rad/s.	37
5.2	Block diagram of the nonlinear model.	38
5.3	Block diagram of the controller.	39
6.1	Yaw-rate response for velocity 5 m/s and 20 m/s for different PI-tuning parameters.	45
7.1	Pole placement of the transfer function for the linear single track model. The circle is the zero and the crosses are the poles.	48
7.2	Pole placement of the transfer function for the closed loop. The circles are the zeros and the crosses are the poles.	49
7.3	Yaw-rate response for different velocities with the same PI controller parameters. The yaw-rate reference does not depend on the driver inputs and is set to 0.3 rad/s.	50
7.4	Yaw-rate response for different velocities with the same PI-tuned parameters. Yaw-rate reference depends on the driver inputs, where the steering-wheel angle is set to $\pi/3$ rad.	51
7.5	Step response for a step steering input at speed 10 m/s and steering-wheel angle of $\pi/9$ rad.	52

7.6	Step response for a step steering input at speed 10 m/s and steering-wheel angle of $\pi/6$ rad.	53
7.7	Step response for a step steering input at speed 10 m/s and steering-wheel angle of $\pi/3$ rad.	53
7.8	Lane change at speed 20 m/s without TVDC.	54
7.9	U-turn at speed 20 m/s without TVDC.	55
7.10	Circle at speed 20 m/s without TVDC.	55
7.11	Lane change at speed 20 m/s using TVDC.	56
7.12	U-turn at speed 20 m/s using TVDC.	57
7.13	Circle at speed 20 m/s using TVDC.	57
7.14	Yaw-rate response for an accelerating vehicle with a step steering-wheel input of $\pi/2$ rad.	58
7.15	Torque on each wheel for different types of differential with a step steering-wheel input of $\pi/2$ rad.	59
7.16	Yaw-rate error for a lane change at speed of 20 m/s.	60
7.17	Yaw-rate error for a U-turn at speed of 20 m/s.	60
7.18	Yaw-rate error for a circle at speed of 20 m/s.	61
7.19	Yaw-rate error when the vehicle is accelerating in a curve.	62

List of Tables

4.1	TVDC model parameters.	33
4.2	Chassis model parameters.	33
4.3	Tire model parameters.	33
4.4	Combustion engine model parameters.	34
4.5	Electric powertrain input parameters [4], [14].	34
6.1	PI controller parameters for all velocities.	46
6.2	PI controller parameters for different velocities.	46
6.3	PI controller parameters for different velocities.	46
7.1	Average absolute yaw-rate errors.	62

Acronyms and Abbreviations

ESC	Electronic Stability Control
RWD	Rear-Wheel-Drive
LFS	Lund Formula Student
LSD	Limited Slip Differential
ECU	Electronic Control Unit
TV	Torque Vectoring
CAN	Controller Area Network
YSC	Yaw Stability Control
ABS	Anti-lock Braking System
DBS	Differential Braking System
MTFC	Maximum Tire Friction Circle
TVDC	Torque-Vectoring Double Clutch
COG	Center of Gravity
TS	Tractive System
LV	Low Voltage
OD	Open Differential
RPM	Revolutions Per Minute

Nomenclature

Variable name	Description
δ	Driver steering angle
δ_{ss}	Steady state steering angle
δ_w	Road wheel angle
T_x	Longitudinal torque
$T_{x,tot}$	Total longitudinal torque
$T_{x,rl}$	Longitudinal torque rear left
$T_{x,rr}$	Longitudinal torque rear right
F_x	Longitudinal force at COG
F_y	Lateral force at COG
$F_{y,f}$	Lateral force at front wheels
$F_{y,r}$	Lateral force at rear wheels
M_z	Yaw moment at COG
I_z	Vehicle inertia
Gr	Gear Ratio between motor to wheels
m	Vehicle mass
R	Circular path radius
ψ	Yaw angle
$\dot{\psi}_{des}$	Desired yaw rate
$\dot{\psi}_{upperbound}$	Desired yaw rate, upper bound
$\dot{\psi}_{lowerbound}$	Desired yaw rate, lower bound
$\dot{\psi}_{target}$	Actual yaw rate
α	Lateral tire slip angle
α_f	Lateral tire-slip angle, front wheels
α_r	Lateral tire-slip angle, rear wheels
β	Vehicle slip angle
$\sigma_{v,f}$	Velocity angle, front wheels
$\sigma_{v,r}$	Velocity angle, rear wheels
L	Wheelbase
l_f	Distance from COG to front axle

l_r	Distance from COG to rear axle
l_w	Trackwidth
V	Global velocity
V_x	Longitudinal vehicle velocity
V_y	Lateral vehicle velocity
$V_{w,rl}$	Wheel velocity, rear left
$V_{w,rr}$	Wheel velocity, rear right
C_s	Longitudinal tire stiffness
$C_{\alpha,f}$	Lateral tire stiffness, front wheels
$C_{\alpha,r}$	Lateral tire stiffness, rear wheels
C'_{ml}	Maximum lateral tire stiffness, rear left tire
C'_{mr}	Maximum lateral tire stiffness, rear right tire
R_l	Maximum friction force on left tire
R_r	Maximum friction force on right tire
D	Driving force
K_V	Under-steer gradient
h_g	Height of center of gravity
a_x	Longitudinal vehicle acceleration
a_y	Vehicle lateral inertial acceleration
\ddot{y}	Vehicle inertial lateral acceleration
r_w	Unloaded wheel radius
I_w	Wheel inertia
μ	Tire road friction coefficient
g	Constant of gravity
C	Contribution factor of lateral acceleration
$F_{z,rl}$	Vertical tire load, rear left tire
$F_{z,rr}$	Vertical tire load, rear right tire
$T_{x,rl}^{maxSlip}$	Maximum slip rear left tire
$T_{x,rr}^{maxSlip}$	Maximum slip rear right tire
X, Y	Global vehicle position coordinates
$G_{ol}(s)$	Transfer function for open loop
$G_{cl}(s)$	Transfer function for closed loop

1

Introduction

Since year 2014, every vehicle must have an Electronic Stability Control (ESC) system implemented [1]. ESC is a technology where the vehicle's stability is improved by detecting and reducing loss of traction [1]. However, ESC does not improve the vehicle's cornering abilities during acceleration in curves. It provides torque vectoring by braking to achieve yaw control. The cornering abilities of a vehicle can be improved by applying the right amount of torques to each wheel independently to increase the driving traction force.

Torque vectoring can be applied to different drivetrains. One way to achieve the possibility of torque vectoring is to use an electric motor on each driving wheel. The drawback with this solution could be that electric motors in each driving wheel do not fit for all vehicles because of different restrictions. The double clutch, further discussed in Section 1.1, is designed with restrictions implied and specifications given by the Formula Student car. It differs from other clutches in such way that this one is normally closed, while other clutches are most often normally open [10]. This means that whenever the actuator does not work properly or not at all, the vehicle will still be able to transfer torque to the wheels. Thus, it is interesting to investigate if it is possible to find a torque-vectoring control algorithm made for this specific clutch when applied to rear-wheel driven (RWD) vehicles.

This master thesis was building on an ongoing Master Thesis that was performed by another student in Mechanical Engineering at Lund University [2], where a double clutch was designed for a Formula Student car. This will enable torque control for each driving wheel independently. This type of control is known as torque vectoring [3] and makes it possible to increase a vehicle's performance and safety. It can for example give the vehicle better stability when cornering, whereas understeer and oversteer can be neutralized by the ability to use torque vectoring [3].

The main objective with this thesis project is to design and implement a control algorithm for a normally closed double clutch torque-vectoring device that will be used on a Formula Student car where the driven wheels are located at the rear.

This chapter discusses the areas of torque-vectoring control in vehicles, followed by a background on the Formula Student project and the dual clutch. Previous work within this field is presented and the purpose and goals along with prob-

lem statements of this project are presented. The contribution of the project is also described. Furthermore, the delimitations and assumptions that are made and challenges with this project are described and this chapter is finalized with an outline of the thesis.

1.1 Background

This section provides a description of the background and motive of this thesis.

Lund Formula Student

Formula Student (FS) [6] is a student engineering motorsport competition in Europe where engineering students design, develop, and manufacture a top class single-seat open wheel racing car in just nine months and compete against other universities at competitions all over the world. There are in total 600 universities involved with Formula Student. The competitions consist of static and dynamic events, where the static events contain tests in, e.g., engineering design, cost and sustainability, technical and safety scrutiny, whereas for dynamic events the tests deal thoroughly with, e.g., vehicle maneuverability on different road-paths and vehicle endurance [5]. There are multiple events held worldwide every year, where about 50 to 150 teams attend to compete. The goal with FS is to give students practical insight and experience working in project-based teams and gain knowledge within the area of vehicle dynamics in general [6].

Lund Formula Student is a Formula Student course held at Lund University [5] and it has 13 years of experience and has built a total of ten cars. In many years, the LFS team has been building a hybrid car with a monocoque chassis with combustion engine, which received many trophies and that specific car ended up at second place in the UK 2010. The monocoque-chassis technique continued until 2015, when they started to build a chassis out of a steel space frame instead. This technique is simpler and more reliable to manufacture. It has been continuously used throughout the years since. The goal for 2020 is to build a fully electric car. [6]

The team behind the Lund Formula Student project for which the control algorithm is implemented, consists of students from Lunds tekniska högskola (LTH). The team's work structure is divided into projects, which are within the areas of circuit boards, TS control, LV system, and mechanics [6]. The different subteams are divided into three groups called the chassis, electronics, and powertrain. All students work iteratively to produce next year's LFS car. The results of this thesis project are planned to be reused for the competition in 2021, depending on what type of powertrain that will be implemented that year. The competition spot is decided every year early January after participating in an engineering quiz competition deciding if the FS team will be able to compete. Those who have the best results, get to come to that year's competition [7].

Dual Clutch

The control algorithm is developed to fit a dual clutch. The dual clutch is a mechanical device, also known as a electro-hydraulically actuated clutch with no differential gears [4]. This concept uses two independently controlled clutch packs connected to each rear wheel, which means that the wheels are able to rotate with different speeds. The principle is to achieve individual torque control at each wheel and thus make torque vectoring possible [4]. The torque can be sent from the slower wheel to the faster wheel. When driving in a corner, the outside wheel can have a fully closed clutch, which means that no clutch slip can occur. At the same time, the inner wheel clutch is partially open and thus slipping, and is able to transfer a certain amount of torque. If the input torque, i.e., the total torque required by the driver, is known, the outer wheel torque can be calculated. Since it is possible to achieve torque allocation on the wheels the yaw rate can be controlled. This is used in the control algorithm. The dual clutch seems to have higher potential in improving vehicle performance, and thus it is interesting to investigate this aspect further on a RWD car to come to a conclusion.

This specified concept used in the dual clutch, is not new as it is very similar to the GKN Twinster [4]. The GKN Twinster is used on cars with on-demand AWD on the rear wheels. Although the dual clutch is built in a different way, it is also applied to a rear-wheel driven car and makes these aspects worth to investigate. The torque-vectoring algorithm on the dual clutch, can be used on other types of ground vehicles. The dual clutch is expected to work with both combustion and electric engines. Both clutches can also be disconnected simultaneously, so there is a possibility to use the concept not only for torque vectoring but also for launch control, which means that the driver has control of the RPM at the start of the driving, which allows for a whole new market for the dual clutch.

For further detailed reading about this topic, see the Master Thesis by Sven Kalkan [4].

1.2 Previous Work on Torque Vectoring

The area of torque vectoring has earlier been studied by others and the results can give a sense of understanding within the area. Antunes, [19], presented his work where he explained how he solved the problem by mainly considering a linear single track model. The model is also described in Section 2.3 and will later also be used in this thesis. Antunes uses the linear model to simulate and estimate vehicle behavior, where he controlled the system by ΔT , which is the difference in torque on the left and the right rear wheel. This implicates that he did not use torque allocation, something that is done in this thesis. Torque allocation means that the torque moment is specifically divided and allocated to the wheels. Antunes only considered the difference in torque and did not care about the allocation to respective wheel. Further on, he showed how different velocities gave different poles and zeros in a

root loci diagram. This implies that different velocities required different PI tuning of the control parameters. Antunes [19] also showed that a PI controller could be used to get good control for the linear model.

Torque-vectoring algorithms can be implemented in various ways. One question can be what reference values should be used and how they should be calculated. Mikulas, Gulan and Takacs, [20], used three reference variables, namely the longitudinal velocity, lateral velocity, and yaw rate. The lateral and longitudinal velocity references, for instance, depend on the current speed, the motor torque requested by the driver, and the maximum allowable speed together with other variables. The yaw rate depends, among other things, on the vehicles geometry, the vehicle current longitudinal velocity, and the steering-wheel angle. This type of yaw rate is commonly used in various articles [20] [21]. Further on, Mikulas, Gulan and Takacs presented two controllers based on model predictive control [20]. Another article proposed to use yaw-rate control realized by both active differential and active roll control system [22]. E. Siampis, M. Massaro, E. Velenis [23] combined yaw stabilization and velocity regulation to mitigate terminal under-steer using an LQR controller together with a backstepping controller to provide drive-torque input. The authors used a linear single track model as a reference model in steady-state cornering. The yaw was controlled by interpreting the drivers steering-wheel-angle command as the desired path radius, assuming the vehicle velocity was constant. M. Canale, L. Fagiano, M. Milanese, and P. Borodani [25] used a linear single track model to control the yaw moment. The controller used an internal model control technique in the feedback loop. The controller further used a feedforward loop driven by the steering-wheel angle. Another variant of yaw-moment control is to instead use a two-degree-of-freedom linear-parameter-varying controller [26]. The controller design was based on Lyapunov functions.

Worth notice is that the different articles mentioned previously use different assumptions and delimitations.

1.3 Purpose and Goals

The main motive of this thesis is to design and evaluate a control algorithm for a double clutch with torque-vectoring capabilities. This is made for a Formula Student car with a normally closed twin-clutch. Since the race-car performance is about maximum velocity under a given period of time, the main goal is to design the controller in such way that the torque distribution at the rear wheels improves the vehicle's stability while cornering. The goal is to make a virtual verification of the control algorithm by simulation in MATLAB.

Problem Statements

Questions to be answered throughout the project are the following:

- Can a Formula Student car designed with a torque-vectoring double clutch benefit compared to a Formula Student car, which is normally designed with limited slip differential, with regards to cornering capabilities?
- Can this type of control help avoiding over- and under-steering?
- How can this concept, where a double clutch torque-vectoring device is applied on a RWD racing car, improve the cornering capabilities in general?

1.4 Contribution

This thesis project contributes with knowledge about control of vehicle dynamics and give a sense of how control strategies can be used to improve a vehicle's driving behavior. The main goal when it comes to the development of knowledge is to advance the technical skills for designing and implementing control algorithms for torque vectoring in race cars. It also contributes to a better understanding of how torque vectoring affects the driving of the car in different situations, given that the car is RWD, and how large influence under-steer as well as over-steer have on the cornering capabilities.

Furthermore, the solution of the considered problem can contribute to new more advanced technology for increased speed while cornering with RWD racing cars. It can also be further developed to be applied on different types of wheel-driven cars in general and provide vehicles with more safe and robust driving behavior for benefit of the society.

1.5 Delimitations and Assumptions

Vehicle dynamics exhibit a wide range of behavior that are important factors to consider to enable the vehicle to drive safely under different road conditions, such as tire temperature, air resistance, road-bank angle, inclination angle, and camber angle. However, in this thesis these and other parameters are excluded. The controller will only take the yaw moment and lateral acceleration into consideration. Sensors for body acceleration, wheel velocity, steering wheel angle and body yaw rate are all available to measure. From these quantities, the body velocity can be calculated. The vehicle operates under a wide range of conditions, which means that the control system needs to guarantee stability and robustness on all roads. However, the road condition will be assumed to be dry asphalt, and thus assuming a constant road friction. Further, longitudinal tire slip and negative torques are taken into account when implementing the controller. The Formula Student Car is rear-wheel driven with an active differential and has front steering wheel system. Wheel self-aligning torque is neglected.

Another limitation is that no error handling, i.e., if a sensor fails, will be implemented and thus, no analyze of possible errors that can occur during experiments in real life will be made.

Note that the model used for control described in this thesis does not take external disturbances into account, such as car accidents, animal incursions and cross-winds or other environmental influences.

1.6 Challenges

From a control theory point of view, one of the challenges that is rooted in the difficulty of vehicle stability is the nonlinear dynamics. A general framework for control of nonlinear systems is lacking, even though there is a lot of mathematical tools for steering a system to a desired state.

Other challenges depend on the many vehicle states that can be affected by controlling one specific state because of the coupled dynamics. For example, when controlling the yaw rate, the vehicle velocity can be affected. Thus, it will be important to always analyze other signal behaviors than just yaw rate when developing the control algorithm. Path following for nonlinear systems are challenging as the road dependence on many tire-force related parameters also affects the system performance.

1.7 Thesis Outline

Chapter 1 contains an introduction to the important aspects for enabling torque vectoring in cars for improving vehicle performance. It contains a short description of the background of this thesis, including what the purpose and goals are and how the results contribute to state-of-the-art. Previous work on torque vectoring is presented and delimitations and assumptions are stated. Furthermore, a presentation of challenges is given.

Chapter 2 gives a description of vehicle dynamics and the important components needed for the simulation model.

Chapter 3 describes torque vectoring and its impact on vehicles behavior and how different types of differential affect vehicle performance.

Chapter 4 presents the model parameters and the vehicle input signals that are used for the controller.

Chapter 5 presents the vehicle performance criteria stated by the FS team and explains the available sensors and their functions. The control strategies used to design and implement the controller is described. Further, a schematic figure of the MATLAB simulation model is shown for the different models.

Chapter 6 presents the main working principle of the controller parameter tuning.

Chapter 7 presents the results from the simulation models and verification and validation of the system on a given vehicle model simulation.

Chapter 1. Introduction

Chapter 8 includes a discussion based on the results from the control algorithm. It also includes discussion about limitations and improvement as well as stability and safety on roads. Future work is presented. Finally, conclusions with regards to the simulation results and discussions made in the previous chapter are stated.

2

Vehicle Dynamics

In this chapter, a brief introduction to vehicle dynamics is presented. The vehicle coordinate system that will be used throughout this thesis is presented, along with an explanation of the used model equations. Furthermore, the tire behavior and how the cornering abilities are related to a car's maneuvering on the road, as well as how vertical tire loads affect the maneuverability are explained.

2.1 Vehicle Axis System

The vehicle axis system contains three dimensions. The coordinate system that is commonly used in vehicle dynamics and will be used throughout this thesis is seen in Figure 2.1. The x-axis represents the forward or longitudinal moving direction of the vehicle and the y-axis represents the sideways or lateral moving direction. The y-axis is perpendicular to the x-axis and is defined as positive when it points to the left of the driver. The z-axis describes the vertical direction pointing towards the ground and will mainly be used to describe normal loads. The rotational axis is the z-axis in the center of gravity (COG). It describes the orientation of the vehicle and is represented by the yaw rate ψ . The yaw rate describes a vehicle's angular velocity around its COG. Observe that the xy-plane moves as the vehicle rotates around the z-axis in the COG. The yaw rate is positive for a left-hand turn.

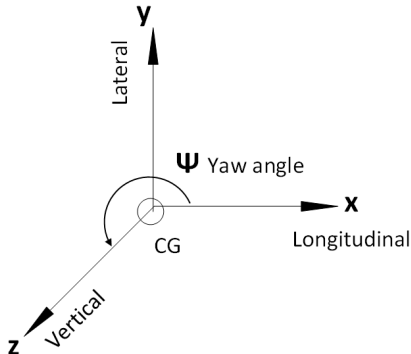


Figure 2.1: The vehicle axis system.

2.2 The Tire Behavior

The tires have a significant impact on the vehicle dynamics, since they enable the vehicle to accelerate, maintain a specific velocity, and brake thanks to friction. By rolling on the road, the tires can also minimize the necessary traction force. Another contribution is that of lateral friction, which enables steering and side stability of the vehicle.

This observation means that the better tire grip, the better possibility to accelerate or brake. However, the tire grip, besides many other factors, also depends on the normal force generated by the vehicle's weight. The normal force on each tire changes when the vehicle is accelerating, braking or cornering. In other words, there are many factors that can affect the vehicle behavior because of all the factors that can affect the tire functionality.

When the tires lose their grip, longitudinal tire slip or/and lateral tire slip will occur. The first mentioned is when the driven wheels do not have the same velocity as the vehicle. This means that the tires are spinning or locking. The lateral slip can be described with the so called slip angle. The slip angle is defined as the angle between the direction of the velocity vector V and the direction the tires point towards when cornering. All equations, (2.1) to (2.23), in the rest of this section are taken from "Vehicle dynamics and control" by Rajamani p. 27-30 [8]. The tire slip angle is denoted α and is for the front tires and the rear tires given as

$$\alpha_f = \delta - \sigma_{v,f}, \quad (2.1)$$

$$\alpha_r = -\sigma_{v,r}, \quad (2.2)$$

where δ is the steering wheel angle relative the vehicle longitudinal axis, $\sigma_{v,f}$ and $\sigma_{v,r}$ represent the velocity angle at the front and the rear tires, respectively. The ve-

locity angle is the angle that the velocity vector makes with the longitudinal vehicle axis, see Figure 2.2.

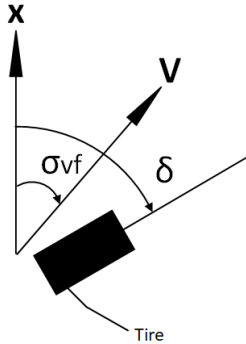


Figure 2.2: Lateral tire slip angle of the front wheel.

The velocity angle is calculated for the front and the rear tires as follows

$$\sigma_{v,f} = \tan^{-1} \left(\frac{V_y + l_f \dot{\psi}}{V_x} \right), \quad (2.3)$$

$$\sigma_{v,r} = \tan^{-1} \left(\frac{V_y - l_r \dot{\psi}}{V_x} \right), \quad (2.4)$$

where V_y is the lateral velocity vector, V_x is the longitudinal velocity vector, l_f the distance from center of the vehicle to the front tires, and l_r the distance from the center of the vehicle to the rear tires.

If the slip angles are equal at both front and rear axles, the car is neutral. However, it is impossible to have a neutral car with the maximum grip on the respective axles for two different slip angles. If the slip angle is bigger at the rear than the front wheels, the vehicle gets under-steered. The opposite, where the slip angle is bigger at the front than the rear wheel, the vehicle is called over-steered. The solution to this is thus to balance the under and over-steering by applying asymmetric torque to the wheels.

The lateral tire forces are described as

$$F_{y,f} = 2C_{\alpha,f} \alpha_f, \quad (2.5)$$

$$F_{y,r} = 2C_{\alpha,r} \alpha_r, \quad (2.6)$$

where $C_{\alpha,f}$ and $C_{\alpha,r}$ denote the cornering stiffness at front and rear tires respectively.

Substituting (2.1) and (2.2) into (2.5) and (2.6), we get

$$F_{y,f} = 2C_{\alpha,f}(\delta - \sigma_{v,f}), \quad (2.7)$$

$$F_{y,r} = 2C_{\alpha,r}(-\sigma_{v,r}). \quad (2.8)$$

2.3 The Single Track Model

There are many ways of describing vehicle dynamics in terms of degrees of freedom. One of the most simplified models is called the single track model, which uses two degrees of freedom [8] and can be seen in Figure 2.3. The two degrees of freedom represent the vehicle lateral position V_y and the vehicle yaw rate ψ , which can be studied in Figure 2.1. The single track model is an interweaving of two wheels with both rear and front wheels as one wheel at each axle. Both variables contribute to longitudinal forces during constant driving, acceleration, and braking. One of the drawbacks with the single track model is its simplified dynamics. The model is a more simple version, representing vehicle dynamics in the linear region. The single track model does not consider the lateral and longitudinal forces on the left and the right tires independently, and thus, only using a single track model will not replace the entire spectrum of vehicle behavior caused by nonlinear dynamics.

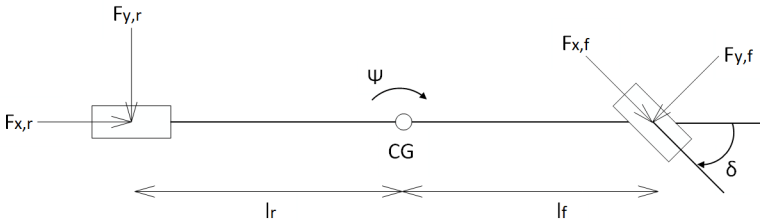


Figure 2.3: The single track model.

The equations of motion that describes the single track model are described in the following.

Equations of Motion

Newton's second law [8] applied on the vehicle motion gives

$$ma_y = F_{y,f} + F_{y,r}, \quad (2.9)$$

where m is vehicle mass, a_y is the inertial vehicle lateral acceleration, and $F_{y,f}$ and $F_{y,r}$ lateral tire forces of the front and the rear wheels, respectively. The term a_y is

affected by both the acceleration the driver is feeling \ddot{y} , which is due to motion along the y -axis, and the centripetal acceleration $V_x \dot{\psi}$. Hence, this leads to the following relation

$$a_y = \ddot{y} + V_x \dot{\psi}. \quad (2.10)$$

The yaw dynamics can be described as

$$I_z \ddot{\psi} = l_f F_{y,f} - l_r F_{y,r}, \quad (2.11)$$

where I_z is the moment of inertia of the vehicle, $\dot{\psi}$ is the yaw rate, l_f the distance from the center of gravity to the front tires and l_r the distance from the center of gravity to the rear tires.

State Space Model

From the relations in Section 2.2 and the equations of motion described in the preceding paragraphs, the following state space model can be written under the assumption that the yaw angles is small, as [8]

$$\frac{d}{dt} \begin{bmatrix} y \\ \dot{y} \\ \psi \\ \dot{\psi} \end{bmatrix} = \begin{bmatrix} 0 & 1 & 0 & 0 \\ 0 & -\frac{2C_{\alpha,f}-2C_{\alpha,r}}{mV_x} & 0 & -V_x - \frac{2C_{\alpha,f}l_f-2C_{\alpha,r}l_r}{mV_x} \\ 0 & 0 & 0 & 1 \\ 0 & \frac{2C_{\alpha,f}l_f-2C_{\alpha,r}l_r}{I_z V_x} & 0 & -\frac{2C_{\alpha,f}l_f^2-2C_{\alpha,r}l_r^2}{I_z V_x} \end{bmatrix} \begin{bmatrix} y \\ \dot{y} \\ \psi \\ \dot{\psi} \end{bmatrix} + \begin{bmatrix} 0 \\ \frac{2C_{\alpha,f}}{m} \\ 0 \\ \frac{2C_{\alpha,f}l_f}{I_z} \end{bmatrix} \delta. \quad (2.12)$$

The relation (2.12) is a commonly used single track model within vehicle dynamics modeling [8]. However, it has a lack of information when it comes to torque-vectoring dynamics. To be able to estimate how torque vectoring affects the yaw rate, an input signal that depends on the torque difference on the rear wheels is introduced as in [19]. The new part that is added to the right-hand side of the state space function in (2.12) is

$$\begin{bmatrix} 0 \\ 0 \\ 0 \\ \frac{1}{I_z} \end{bmatrix} M_z = \begin{bmatrix} 0 \\ 0 \\ 0 \\ \frac{1}{0.02I_z} \end{bmatrix} \Delta T. \quad (2.13)$$

The constant 0.02 is introduced when replacing the vehicle yaw moment, M_z , with the difference in torque on the rear wheels, ΔT , since the relation between the variables is as follows [19]

$$\Delta T = \frac{r_w}{l_w G_r} M_z, \quad (2.14)$$

where G_r is the gear ratio from the motor to the wheels. For the Formula Student vehicle, (2.14) results in the following relation [19]

$$\Delta T = \frac{0.22}{1.19 \cdot 8.48} M_z = 0.02 M_z. \quad (2.15)$$

2.4 Under-Steer Gradient

To see whether a vehicle is understeered or oversteered, one can measure the under-steer gradient, which is formulated as (p. 209 in [8])

$$K_V = \frac{l_{rm}}{2C_{\alpha,f}L} - \frac{l_{fm}}{2C_{\alpha,r}L}, \quad (2.16)$$

where L denotes the wheelbase of the vehicle, i.e., $L = l_f + l_r$.

If the front slip angle is higher than the rear slip angle, the vehicle tends to under-steer. As for the opposite, when the rear slip angle is higher than the front slip angle, the vehicle over-steers. This implies that when the slip angles are equal at the front and at the rear tires, the vehicle has a neutral steering and thus is in equilibrium. This sums up in the following conclusions (see p. 57 in [8]):

1. If $K_V > 0 \implies \alpha_f > \alpha_r$, which means that the vehicle is understeering.
2. If $K_V < 0 \implies \alpha_f < \alpha_r$ the vehicle is oversteering.

The under-steer gradient is implemented in the desired yaw rate equation, which is further described in Section 5.4.

Vertical Tire Loads

If the wheel axles are loaded with a moment, the contact patch between the tire and road must be able to transfer forces. The available friction between tire and road, μ , decides the maximum moment, M^{max} , on the wheels. The relation is presented as

$$M^{max} = r_w F_x = r_w \mu F_z. \quad (2.17)$$

When introducing longitudinal acceleration, the vertical load shifts towards the rear increasing the vertical load on the rear tires and decreasing the load on the front tires. As for decelerating, i.e., braking, the vertical load increases on the front tires but decreases on the rear tires. However, when a vehicle corners at lateral acceleration, load transfer occurs between the left and the right wheels [12]. Both results affect the distribution of normal forces on each wheel.

The following relation for the left rear wheel and the right rear wheel describes the vertical loads on the tires with the assumption that there is no suspension between the body and the wheels,

$$F_{z,rl} = \frac{mgl_f}{2(l_f + l_r)} + \frac{ma_x h_g}{2(l_f + l_r)} - \frac{may h_g}{2t_w}, \quad (2.18)$$

$$F_{z,rr} = \frac{mgl_f}{2(l_f + l_r)} + \frac{ma_x h_g}{2(l_f + l_r)} + \frac{may h_g}{2t_w}, \quad (2.19)$$

where h_g is the height of the center of gravity [11].

In order to limit the amount of torques, we need to control the longitudinal slip and the maximum allowable engine torque (see Section 5.4). This is done by introducing an upper limit and a lower limit. The maximum longitudinal slips on each rear wheel are functions of the vertical tire load $F_{z,rj}$ (r denotes rear wheels and j denotes left or right), tire-road friction coefficient μ and wheel radius r_w . Given (2.17), (2.18), and (2.19), the following maximum longitudinal slip is obtained

$$T_{x,rl}^{maxSlip} = r_w \mu F_{z,rl}, \quad (2.20)$$

$$T_{x,rr}^{maxSlip} = r_w \mu F_{z,rr}. \quad (2.21)$$

2.5 Global Coordinates

Since the single track model is based on body-fixed measurements of position error relative to the road, a global representation of the trajectory must be obtained in order to visualize the paths traversed by the vehicle in a XY-plot. Hence, the body-fixed coordinates must be converted into trajectories in inertial space. The position of the vehicle in global coordinates is given by the relations from Rajamani (p. 26 in [8])

$$X = \int_0^t V \cdot \cos(\psi + \beta) dt, \quad (2.22)$$

$$Y = \int_0^t V \cdot \sin(\psi + \beta) dt, \quad (2.23)$$

where V is the resultant velocity defined later in (5.5) and β is the vehicle slip angle and is assumed to be close to zero.

3

Torque Vectoring

This chapter gives a brief presentation of torque vectoring and how its function applies to vehicles and can improve a vehicle maneuver.

A high tire-road friction coefficient could be able to provide enough lateral force that is required by the vehicle to follow a curve, but low tire-road friction coefficients and high velocity can lead to insufficient lateral tire forces. This means that when driving at high speed, the vehicle could become unable to follow the motion that is requested by the driver and thus when cornering in a curve, a large curve radius is needed to enable the vehicle to follow the radius in a safe way. These are situations where torque vectoring can be applied to the wheels.

Torque vectoring is a technology used for torque distribution to the vehicle's wheels [8]. It is applied on driving wheels instead of using the brake systems to control the yaw rate and lateral acceleration. In a four-tire drive system, the torque is transmitted to all four wheels and for a rear-tire drive system, the torque is instead transmitted to the two rear wheels. When a vehicle is exposed to loss of traction, e.g., in off-road routes, longitudinal tire forces need to increase in order to maintain the vehicle maneuver in a stable way.

This is made by transmitting torque to the wheels. The applied torque can enable stability in situations where the vehicle is under or over-steering. When torque is transmitted, it means that the longitudinal tire traction force is generated at the respective tire to aid the forward longitudinal moving direction of the vehicle. However, it is of importance to mention that at, e.g., slippery roads, the torque transmitted to the wheels does not stop a vehicle. This is determined only by the brake system used in the vehicle and it is one of the good assets with torque-vectoring algorithms.

During cornering, the vertical tire loads will be distributed differently compared to when the vehicle is keeping a constant forward speed. Because of this, each tire will get a different grip characteristics. For example, the inner tires will get less grip while the outer tires will get higher grip. This fact can be utilized in torque

vectoring. Better tire grip implicates that the car has a better chance of accelerating and braking without making the vehicle to spin or slip.

Maximum Tire Friction Circle

In order to understand the torque-vectoring approach, it is beneficial to understand the Maximum Tire Friction Circle (MTFC) [12]. The MTFC describes the relation between the maximum tire friction force, the driving traction force (also known as the longitudinal traction force) and the maximum cornering force of the left and the right wheel when a vehicle is cornering. The sum of driving traction force and cornering force can never be bigger than the MTFC. The MTFC depends on the normal force for each tire. While a vehicle is turning left, the lateral acceleration causes the normal load on the left tire to decrease, which in turn causes a decrease of maximum friction force, R_l . In the same way, the lateral acceleration gives more normal load to the right tire and causes the maximum friction force, R_r , to increase. Figure 3.1 and Figure 3.2 show MTFC for a left turn [12].

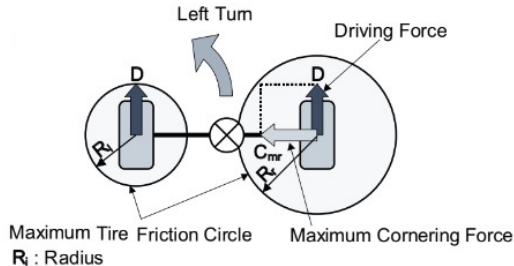


Figure 3.1: The maximum tire friction circle without torque vectoring [12].

Without torque vectoring, the scenario shown in Figure 3.1 can occur. In Figure 3.1, it is shown that the driving traction force D is equal on both wheels and that only the right wheel generates a cornering force C_{mr} . This is because the left MTFC is only used for longitudinal driving traction force. To generate some cornering force from the left tire, it is therefore necessary to decrease the driving traction force on the left tire. Since the right MTFC is bigger, it is possible to increase the driving traction force by applying more torque to that tire and keep cornering force from the right tire. In that way, the desired velocity can be kept as well as improving the cornering behavior.

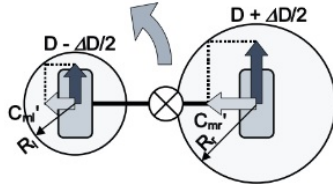


Figure 3.2: The maximum tire friction circle with torque vectoring [12].

When the torques applied to the wheels are independently controlled, the new driving forces are $D - \Delta D/2$ on the left tire and $D + \Delta D/2$ on the right tire. This implies that each tire can generate maximum cornering force C'_{ml} and C'_{mr} . The total cornering force is then increased, while the driving force remains. This is shown in Figure 3.2. Observe that the friction circles are mostly used for explaining and understanding tire friction forces. Most often tires have a higher value of lateral friction compared to longitudinal friction. Because of this, the tire friction circles are more commonly formed as ellipses, with a bigger radius in the lateral direction.

The advantage with torque vectoring is that it aims to reduce lateral slip and increase the usage of friction potential at the tires, which improves the driving traction force of the vehicle. This is all without affecting the driving comfort and not allowing the vehicle to decelerate. However, when a vehicle is cornering, the outer wheels will have to travel a longer distance than the inner wheels. This is because the outer wheels have a larger curvature than the inner wheels and thus must spin faster than the inner wheels to enable the vehicle to follow the curve. Because of this, the outer tire will need a higher velocity to keep up with the inner tire. To solve this problem, differentials are used to enable left and right wheels to spin at different speeds.

Different Types of Differentials

To achieve different torques on the right and the left side, there are various types of differentials used in vehicles [8]. A differential is a mechanical component that allows the inner and outer tire to have different speeds while cornering. Depending on the vehicle drive system and the design of the differential, the torque can be distributed equally or unevenly to the front and the rear axles, but also to the left and right front or rear wheels. An open differential distributes torque equally to the right and the left tire, independently of the tire grip on the wheels [8]. The tire with the least tire grip will decide the amount of torque distributed to both wheels. For example, if one of these tires loses its grip, i.e., if it enters a slippery surface, it will not require much torque to spin at a desired velocity. The other tire will receive the same amount of torque since the open differential splits the torques equally and will not be able to generate maximum longitudinal traction force.

A locking differential is an improvement of the open differential [8]. With the locking differential the driver can operate a switch to lock the wheels together. In that way, both wheels together will receive the total torque and the tire that is not on a slippery surface can get enough torque to provide the longitudinal traction force. The wheels in this case are rotating with the same speed.

A third type of differential is the limited slip differential (LSD) [8]. This type of differential initially allows equal slip between the tires. In the LSD, a clutch progressively locks the wheels together but the wheels can still rotate at different speed. It does not necessarily mean that the tire velocity is the same on both wheels. When the tire velocity difference is big enough, the two wheels will get locked and the advantage of this is again the provided longitudinal traction force. The disadvantage with LSD is, when driving with high speed and one tire starts to slip, that the equal torque transfer to the wheels will make the car slower [8].

3.1 Yaw Stability Control

Yaw stability control (YSC) systems are developed to control a vehicle's yaw rate [8], which is the angular velocity around the vehicle's center of gravity. Yaw control systems prevent vehicles from undesired spinning and drifting. In other words, the goal is to restore the yaw rate of the vehicle as much as possible to the expected motion from the driver. Vehicle yaw velocity can be affected by the steering tire angle but also by applying different amount of torques on the left and the right rear tire [8].

Different Ways of Controlling Torque Transfer using YSC

There are three different types of differentials that can improve the yaw stability. One is the differential braking, which utilizes the anti-lock braking system (ABS) [8]. This type of control system, which is called differential braking system (DBS) [8], is applied when a vehicle does not have active differentials, i.e., differentials that do not have the function of applying differential torque. One of the drawbacks with this type of differential system is that the vehicle slows down and may not give the desired longitudinal response requested by the driver if used during vehicle acceleration. The other type is a controlled LSD and has been described in the previous section. The LSD will increase torque to the inner tire but not the outer tire. Drawbacks with using this control is that torque transfers only occur from the faster driving tire to the slower one. Finally, the third type is the active torque distribution where a twin-clutch torque transfer differential is used [8]. This differential gives the ability to independently control the drive-torque distribution to each driven tire, without a reduction in vehicle acceleration.

The type of torque distribution implemented in this report is based on the last mentioned, the twin-clutch torque-transfer differential, on each rear tire. This

method is thus more efficient in theory, when cornering, than the differentials mentioned previously [8].

4

Model Parameters and Sensor Signals

The model parameters used for the control design and the available sensor signals are presented in this chapter.

4.1 Data Collection

The measurements from available sensors and the model data used in this project are acquired from the Formula Student car and were provided by the LFS team. These are as follows:

- maximum combustion-engine torque,
- yaw rate,
- vehicle acceleration,
- wheel velocities,
- steering wheel angle,
- data concerning vehicle body.

Further specified parameter values provided by both the LFS team and Borg-Warner can be seen in Section 4.2.

The maximum combustion-engine torque required by the driver is estimated as seen in Figure 4.1 and it represents the torque limit allowed for the engine. The plot shows the maximum engine torque as a function of angular speed.

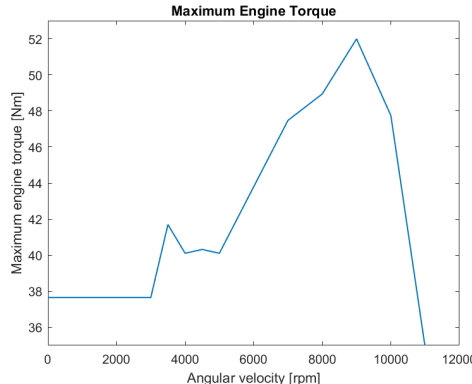


Figure 4.1: Maximum combustion-engine torque on the crankshaft.

The mapping between driver steering angle and the road wheel angle is provided by BorgWarner and the driver steering angle is positive for a left-hand turn, i.e., $0 < \delta < \pi$. The wheel velocities are given directly from a transducer mounted on the car.

Sensors

The torque-vectoring algorithm can be implemented in many ways but the choice of strategy depends on available sensors. The onboard sensors that are available and implemented in the Formula Student Car are gyroscope, accelerometer, wheel velocity sensor, sensor for steering wheel angle, and engine motor torque. In this section, the objective is to describe what they measure. Since the Formula Student car is not yet built, a visualization can not be shown of the placement of the sensors mounted onto the Formula Student car.

Gyroscope Gyroscopes are essential for measuring the angular velocity in yaw, pitch, and roll and can be used in control systems for maintaining orientations. The gyroscope gives velocity in yaw, pitch, and roll.

Accelerometer The accelerometer is a mechanical device, which gives measurements of the vehicle acceleration in both x- and y-direction.

Wheel Speed The wheel speed sensor measures the wheel velocities in m/s.

Driver Steering Wheel Angle This sensor is fully electronic and senses the rotary position of an activator mounted on the sensor [16].

4.2 Vehicle Model Parameters

The following Tables 4.1, 4.2, and 4.3 show the model parameters for the TVDC, vehicle body, and tire. The model parameters are provided by the Formula Student and BorgWarner teams.

Table 4.1: TVDC model parameters.

TVDC stiffness	0.004 Nm/rad
TVDC damping	400 Nm/(rad/s)

Table 4.2: Chassis model parameters.

Vehicle mass	310 kg (including driver)
Vehicle inertia	195.69 kgm ²
Wheelbase	1.59 m
Trackwidth	1.19 m
Height of the center of gravity	0.3 m
Center of gravity	9.82 m/s ²
Mass distribution	0.475
Distance from center of the vehicle to front wheels	0.756 m
Distance from center of the vehicle to rear wheels	0.835 m
Lateral load transfer ratio front	0.475
Longitudinal load transfer delay	0.1 s
Lateral load transfer delay	0.1 s
Air resistance factor	0.3991

Table 4.3: Tire model parameters.

Tire radius	0.22 m
Tire inertia	0.24 kgm ²
Tire to road friction coefficient	0.90 [7]
Tire longitudinal stiffness	5 N
Tire lateral stiffness front	1500 Nm/rad
Tire lateral stiffness rear	1500 Nm/rad
Rolling resistance coefficient	0.015
Brake stiffness	0.003 Nm/rad
Brake damping	300 Nm/(rad/s)

The cornering stiffnesses at both front and rear wheels are set to 1500 Nm/rad, since this is compatible with the vehicle model provided by BorgWarner. The ac-

tual cornering stiffness is much less for the Formula Student car. To represent dry asphalt, the tire to road coefficient is set to 0.90 [7].

The TVDC is planned to be used for both a combustion engine and an electric engine. For the test cases in this report, a combustion engine is used and the model parameters are shown in Table 4.4.

Table 4.4: Combustion engine model parameters.

Combustion engine torque lag	0.1 Nm
Combustion engine inertia	0.2 kgm ²

The electric motor that is planned to be used year 2020 is an EMRAX 228. For detailed information, see Table 4.5.

Table 4.5: Electric powertrain input parameters [4], [14].

Engine	EMRAX 228
Max power	100 kW @ 5500 RPM
Max torque	230 Nm @ 5500 RPM
Number of gears	4

5

Control Strategy

This section provides an explanation on how the control-system design is performed based on given model parameters. The vehicle performance criteria are described taking the given sensors mounted on the Formula Student car into consideration. Three different model strategies are developed and a MATLAB simulation model scheme for the torque-vectoring algorithm approach is presented.

5.1 Vehicle Performance Criteria

The system requirements and the performance criteria for the Formula Student car are to enable effective cornering abilities on dry roads. The improvement between using a LSD or TVDC clutch lies in the accelerating capabilities in a curve. The previously developed Formula Student cars have been using LSD clutches and a recurring problem when competing has been that the car tends to under-steer when accelerating in curves. Thus, the desired improvement, which is noted in different driving modes with LSD, is to enable the tires with enough grip when accelerating in a curve, meaning that the potential is in stabilizing the car when it enters a curve. This can be solved using torque vectoring (TV). With TV, the car can be maneuverable and faster in slalom and turns. TV also enables stability and trust in the driver.

5.2 Modeling

The aim with modeling the system is to, early in the design phase, reveal the effects of vehicle dynamics behavior before the prototype is complete. The control design has been developed in MATLAB/Simulink environments. The control algorithm is implemented using blocks in order to be able to automatically convert the algorithm into C-code. The reason is to later be able to use the control algorithm in ECU's provided by BorgWarner. The conversion will be done through a tool called TargetLink [17]. BorgWarner's Simulink model, which is based on vehicle simulation software, has been available for control development.

The algorithm will in an actual implementation depend on a so called CAN-bus where all essential measured values from the vehicle will come from. For this project, simulated measurements have been used instead. The measurements will be used to estimate the desired behavior of the vehicle and thus give a reference model. The output from the reference model will be used to measure the control error. The error will then be used as the input to the developed controller, where the torques will be calculated and further distributed to each clutch into a vehicle model.

Throughout this thesis, a visual validation and verification test of the control algorithm has been made based on a vehicle simulation model provided by Borg-Warner. An error analysis using quantitative measures has been made to further confirm the stability of the developed control algorithm, see further description in Section 7.3. A final validation will be made on the actual vehicle in order to control all failure conditions, in winter 2020. The final validation is not presented in this thesis.

5.3 Different Modeling Strategies

In this section, different modeling strategies are presented. At first, a linear single track model has been developed. The advantage with this model is its simplicity. Thus, it is easy to evaluate if the control structure is suitable or not.

Further on, the controller is verified in two different types of nonlinear models. These are provided by BorgWarner and are described separately later. The control design for the nonlinear models will be slightly changed compared to the linear model.

The relations presented in Section 2 are implemented in MATLAB/Simulink. Simulink uses the MATLAB coding language [17] with an interface where different blocks are chosen from the Simulink library. These blocks are connected and block parameters are assigned. The parameters presented in Section 4.2 are saved in a MATLAB-script. Further, control strategies, necessary calculations and limits needed to implement the control algorithm are described in the following sections.

Linear Single Track Model with PI Controller

The single track model presented in Section 2.3 was implemented in Simulink to have a low complexity model to rely on. Its input signals are, as can be seen in Figure 5.1, the longitudinal velocity, the steering wheel angle, and the desired yaw rate, which are constants. The longitudinal velocity is put to four different values and the desired yaw rate is put to 0.3 rad/s. The steering wheel angle is put to different angles and is converted to the steering road wheel angle by a remapping of the signal. Further on, there is also a control signal input to the single track model. This signal determines the size of the difference in torque, ΔT , on the wheels. Since the single track model is linear, a PI controller is used to compute ΔT , which in turn controls the actual yaw rate, $\dot{\psi}$.

The mathematical formula for the PI controller is

$$u(t) = K_p e(t) + K_i \int_0^t e(t') dt', \quad (5.1)$$

where K_p and K_i are PI gains. Here $u(t)$ describes the control signal that corresponds to ΔT and $e(t)$ is the yaw-rate error.

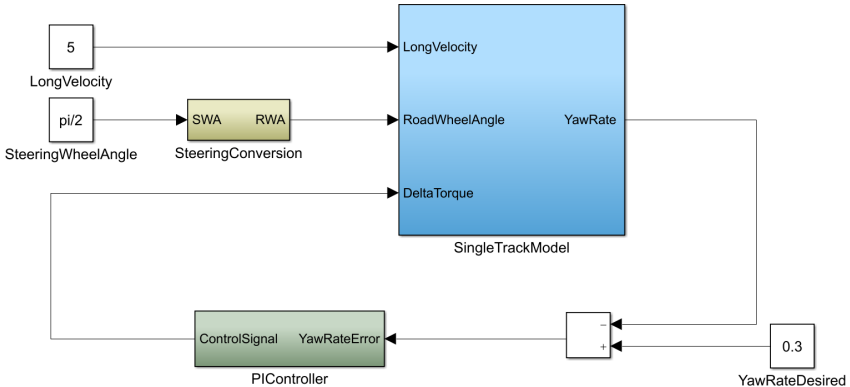


Figure 5.1: Block diagram of the linear model with PI controller for different velocities. In this figure, the longitudinal velocity is set to 5 m/s, the steering wheel angle is set to $\pi/2$ rad, and the desired yaw rate is set to 0.3 rad/s.

Nonlinear Model with PI Controller

In this part, the two nonlinear models provided by BorgWarner are described. The two models both consist of driver signals, a block for the control implementation, and a vehicle model. The goal with this thesis project is to implement the controller. Besides the fact that these models are nonlinear, they also request an independent torque for each rear wheel, i.e., it is not enough to control the vehicle model by only a torque difference as in the linear model.

One of the nonlinear models consists of a vehicle model that is more simple, with no limits on the torques and one is more complex representing a vehicle with a TVDC. The models are described in more detail in the following.

In Figure 5.2, a schematic overview of the vehicle simulation model is shown. The proposed control algorithm is implemented in the controller block.

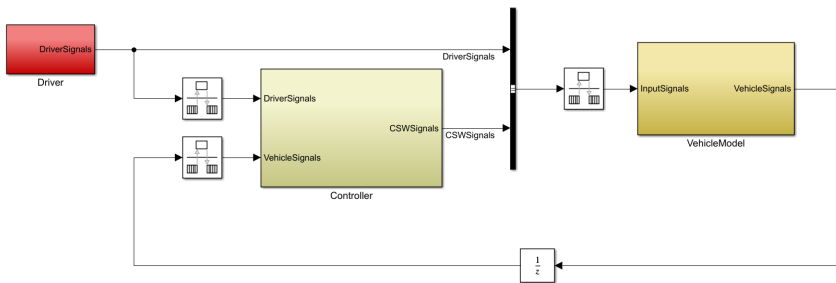


Figure 5.2: Block diagram of the nonlinear model.

The control-algorithm implementation consists of input signals coming from the driver commands, and a controller block where the torque distribution is calculated. As earlier mentioned the nonlinear models consist of a separate vehicle model. The vehicle models differ from each other in the two nonlinear models. The simpler nonlinear model consists of a simpler vehicle model that consists of only a chassis and a tire model. Further on, it only consists of one driver signal, namely the steering wheel angle requested from the driver. The simpler nonlinear model also provides a direct access to the torques applied to the rear wheels without any lag and thus it is easier to control the yaw rate.

The more advanced nonlinear model consists of a vehicle model which is similar to that of the simpler model, and only differs in that it has more complex features added to it. It consists of a chassis model, tire model, and powertrain model. The powertrain model in turn consists of a combustion engine model and a gearbox model. The more advanced vehicle model uses a Torque-Vectoring Double Clutch (TVDC). Here, the driver signals contain parameters such as steering wheel angle, combustion-engine torque, and gear position. The vehicle model can not be visualized to the reader due to confidentiality agreement.

The vehicle model can be described as being similar to a RWD Formula Student car using a twin-clutch, although some input parameters differ. The vehicle model is developed and validated by BorgWarner themselves.

Since a PI controller was sufficient for the linear model, which is shown later in Section 7, a PI controller will therefore also be used as a first attempt for the nonlinear models. The PI controller and torque allocation is implemented in the controller block and an overview of the controller is seen in Figure 5.3.

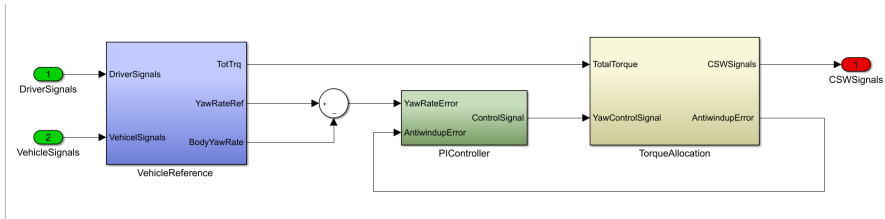


Figure 5.3: Block diagram of the controller.

Whenever the driver tries to steer such that the vehicle deviates from the target, the controller applies adjustments to bring the vehicle back on the right track or to gain a neutral steering. For this case, a desired yaw rate is considered for the vehicle state. The controller then compares the target states with actual measurements and adjusts the vehicle's model input.

The controller is verified using the two nonlinear models mainly. The principles behind the control software block is described in detail in Section 5.5.

5.4 Control Algorithm

This section describes the torque-distribution algorithm needed for the control system implementation and the limits necessary to apply according to the vehicle performance criteria and to improve the stability of the vehicle. The following expression and relations are implemented in the controller block.

Longitudinal Vehicle Velocity

Considering that it is a rear-wheel driven car, the vehicle velocity in longitudinal direction is calculated by taking the average value between the front left and the front right wheel velocity. The expression is

$$V_x = \frac{V_{w,fl} + V_{w,fr}}{2}. \quad (5.2)$$

Because the car is rear-wheel driven, no longitudinal slip will occur on the front wheels. Thus, the vehicle longitudinal velocity computed as in (5.2) will almost always give a correct value.

Desired Yaw Rate

The desired yaw rate for a vehicle can be given by

$$\psi_{des} = \frac{V_x}{R}, \quad (5.3)$$

where V_x is the longitudinal velocity and R is the steady-state radius of a circular path that depends on what steering wheel angle the driver selects. The steady-state

relation between a steady-state steering wheel angle δ_{ss} and the road radius R can be expressed as [8], p. 209,

$$\frac{1}{R} = \frac{\delta_{ss}}{L + V^2 K_V}, \quad (5.4)$$

where V is the global velocity,

$$V = \sqrt{V_x^2 + V_y^2}. \quad (5.5)$$

The desired yaw rate can then be derived to be [8], p. 209,

$$\dot{\psi}_{des} = \frac{V_x \delta}{L + \frac{m V_x (l_r C_{\alpha,r} - l_f C_{\alpha,f})}{2 C_{\alpha,r} C_{\alpha,f} L}}, \quad (5.6)$$

and depends on whether the vehicle is under-steered, neutrally-steered or over-steered, as well as it assumes the vehicle to operate as if it is in steady state.

However, if the road-tire friction coefficient is unable to provide tire forces to support a high yaw rate, the yaw-rate relation (5.6) cannot be obtained. This concludes that the desired yaw rate needs to be bounded by an upper and a lower value. The upper bounded value consists of a function of the tire-road friction coefficient and the lower bound value is the negative of the upper bound value [8], p. 211-212, as described by

$$\dot{\psi}_{upperbound} = C \frac{\mu g}{V_x}, \quad (5.7)$$

$$\dot{\psi}_{lowerbound} = -C \frac{\mu g}{V_x}, \quad (5.8)$$

where C is a constant between 0 and 1 and determines the contribution to the total lateral acceleration. In this case, the yaw-rate boundaries will be set as a result of the fact that the lateral acceleration, a_y , is bounded by the tire-road friction according to

$$a_y \leq \mu g, \quad (5.9)$$

where μ is the road-friction constant and g is the constant of gravity. The lateral acceleration is affected by both the acceleration \ddot{y} , which is due to motion along the y -axis, and the centripetal acceleration $V_x \dot{\psi}$. We have the lateral acceleration given in (2.10) and since $\ddot{y} = V_x \tan(\beta)$, we have the following relation [8], p. 211-212,

$$a_y = a_x \tan(\beta) + \frac{V_x \dot{\beta}}{\sqrt{1 + \tan^2(\beta)}} + V_x \dot{\psi}. \quad (5.10)$$

The term $V_x \dot{\psi}$ in (5.10) dominates and if the body slip angle is small, the other two terms contribute only with a small factor. Hence, C can be chosen to 0.85, meaning

that the limit factor is reduced by 15 % to take into account that the first two terms in (5.10) have been neglected in the limits in (5.7) and (5.8).

Eventually, we get the following constraints:

If $|\dot{\psi}_{des}| \leq \dot{\psi}_{upperbound}$ or $|\dot{\psi}_{des}| \geq \dot{\psi}_{lowerbound}$, we get

$$\dot{\psi}_{target} = \dot{\psi}_{des}. \quad (5.11)$$

If $|\dot{\psi}_{des}| > \dot{\psi}_{upperbound}$, the following is obtained

$$\dot{\psi}_{target} = \dot{\psi}_{upperbound} \cdot \text{sign}(\dot{\psi}_{des}). \quad (5.12)$$

If $|\dot{\psi}_{des}| < \dot{\psi}_{lowerbound}$, then we have

$$\dot{\psi}_{target} = \dot{\psi}_{lowerbound} \cdot \text{sign}(\dot{\psi}_{des}). \quad (5.13)$$

The yaw-rate error is calculated as

$$\dot{\psi}_{error} = \dot{\psi}_{des} - \dot{\psi}_{target}. \quad (5.14)$$

Yaw Moment

Since the actual yaw rate will be controlled by a combination of asymmetric torques on the rear wheels, a relation between the desired yaw rate and the requested torques is needed. If the vehicle is rear-wheel driven, it means that all torque will be supplied to the rear wheels. The following relations, (5.15) and (5.16) give a connection between the yaw moment and the torques required from the driver on the left and right rear wheel, respectively, of the vehicle [13], and thus describe the torque distribution that is required by the driver to achieve the requested yaw moment to the left and the right clutch. The relations are approximated to only consider longitudinal forces as

$$T_{x,rl} = \frac{r_w}{l_w} \left(\frac{l_w}{2} \cdot F_x - M_z \right), \quad (5.15)$$

$$T_{x,rr} = \frac{r_w}{l_w} \left(\frac{l_w}{2} \cdot F_x + M_z \right), \quad (5.16)$$

where $T_{x,rl}$ and $T_{x,rr}$ in the case of a rear-wheel driven vehicle are the longitudinal torques on the left rear wheel and the right rear wheel, respectively. F_x is the longitudinal force, l_w is the track width, r_w is the wheel radius, and M_z is the vehicle yaw moment around the z-axis.

However, a relation between the yaw rate and the torques is needed to be able to control with yaw rate as reference value. In order to obtain that relation, a relation

between the yaw moment and the yaw rate is needed. This formula is obtained by taking the derivative of the yaw rate and multiply with the vehicle inertia as in

$$M_z = \dot{\psi} \cdot I_z, \quad (5.17)$$

where I_z is moment of vehicle inertia around the z-axis.

The yaw moment can also be calculated as the difference in longitudinal force multiplied with trackwidth assuming no lateral forces, and since longitudinal force can be converted to longitudinal torques by multiplying with the wheel radius, the following is obtained

$$M_z = \Delta F_x \cdot \frac{l_w}{2} = \Delta T_x \cdot \frac{l_w}{2r_w}, \quad (5.18)$$

which ultimately gives the following

$$\dot{\psi} \cdot I_z = \Delta F_x \cdot \frac{l_w}{2} = \Delta T_x \cdot \frac{l_w}{2r_w}. \quad (5.19)$$

From this, we can derive the difference in longitudinal torque, which is

$$\Delta T = \frac{2I_z r_w}{l_w} \dot{\psi}. \quad (5.20)$$

The expression (5.20) is substituted with yaw moment in (5.15) and (5.16). Finally, the torque allocation is expressed as

$$T_{x,rl} = \frac{T_{x,tot}}{2} - \frac{r_w}{l_w} M_z, \quad (5.21)$$

$$T_{x,rr} = \frac{T_{x,tot}}{2} + \frac{r_w}{l_w} M_z. \quad (5.22)$$

Limits

In order for the control algorithm to work properly and to output torques that are not too high, there are different types of limits that need to be implemented. These are described in the following sections.

Torque Limit Capacity-moment signals are always positive. The twin clutch is not able to set negative torques on the wheels, except for engine brake. What happens is that the clutch determines the speeds on the different wheels and thus, these wheels get different torques, i.e., one with a higher value than the other. In order to allow only positive torques, the torque-vectoring algorithm needs to control the sign of the vehicle yaw moment on the wheels. According to the expressions given in (5.15) and (5.16), the applied torque on the rear wheels cannot be bigger than the torque demand from the driver. The limit is done with a simple dynamic saturation block in Simulink.

Slip Limit The speed is generally around 70 km/h in competitions. In the lower gears such as 1-3, the wheels can spin, i.e., spin on tires to ground, if too much gas is given. It is important that the control algorithm is limited to maximum torque where spin occurs. This is done according to expressions (2.18) and (2.19).

Anti-Windup Limit Whenever a linear controller has been designed under the assumption that its output will affect the plant input directly and unaltered, any input nonlinearity that causes deviation between the controller output and the plant input, will degrade the performance, and stability of the closed-loop system may be lost. Anti-windup compensation is a simple and commonly used modification of a linear controller, aiming at retaining stability and most of the performance in such a system [18].

Since the control system under some conditions gives saturating inputs to the vehicle model, the control saturation aspects need to be considered when implementing a control system. Therefore, an anti-windup is used in the feedback loop to prevent the integrator part in the PI controller from growing large and cause overshoots and limit cycles during the rise. By this, stability and most of the performance in the system can be retained [18]. A good thing with having an anti-windup in the feedback loop is that it leaves the loop unaffected when there is no saturation values.

There are different types of anti-windups. The one used here is an anti-windup employing a time-tracking constant [18]. Feedback of the difference between the controller output and the estimated plant output is used as an error signal and sent back to the controller. When the plant is not saturated, the error signal is zero and has no impact on the controller. When the plant is saturated, the integrated error signal increases and the extra anti-windup feedback loop to the controller makes the I-part stop growing.

5.5 Controller Implementation Aspects

The vehicle operates under a wide range of conditions, which means that the control system needs to guarantee stability and robustness on different roads and need to handle physical limitations of actuators and tires. Physical limitations mean limitations coming from values that cannot change with desired rate. To reach the ultimate level of safety and driving comfort in a vehicle system, the controller needs to know the drivers required motion. If the controller has information about the driver's states and intentions, it can be better tuned. Since the controller in a vehicle, from a more technical point of view, potentially can react faster and more precise than a human driver, its potential to improve the vehicle stability margin is high. The objective with the controlled twin-clutch differential is to improve vehicle performance by means of an asymmetric distribution of the driving torque to the wheels when accelerating in a corner, without making the vehicle slower.

The system design aims to control the yaw rate. The desired yaw-rate reference is computed in the linear region based on the steering wheel angle, vehicle speed, and under-steer gradient according to (5.6). The yaw-rate error is calculated as the difference between the actual vehicle yaw rate and the desired yaw rate according to (5.14), and is used as an error signal input to the PI controller. The desired yaw rate is limited as seen in (5.11), (5.12), and (5.13).

Since the vehicle model is nonlinear, it is expected to behave differently in various states. For example, its behavior can depend on the velocity. Therefore a pure linear PI controller is not expected to work properly for all velocities. To solve this, gain scheduling [27] will be used. When using gain scheduling, the controller have different tunings depending on the different states. The vehicle velocity is the main scheduling parameter. The vehicle velocity is put to 5 m/s, 10 m/s, 15 m/s, and 20 m/s, for which different parameter tunings are established. The gain scheduling is implemented with a simple if-statement block together with an if-action block in Simulink.

Further, the control signal is used when calculating the torque distribution, in the TorqueAllocation block. The relation used for substituting the yaw-rate error into the difference in torque is seen in (5.20). The torque distribution is then input to the vehicle model according to (5.21) and (5.22), but with M_z replaced with the control signal.

Since the torque-distribution expression implicates a differentiator part of the controlled yaw-rate error, the static error will return. From a control point of view, the differentiator is not ideal. A solution to this kind of problem is to remove the amplifications of noise in the measurement signal and the elimination of the static error can thus be regained. Instead, the output from the controller was set to be the input in (5.15) and (5.16).

The test cases are divided into linear and nonlinear model, where the vehicle model varies as described in the previous section. The different subsystems need to communicate with each other in order to improve the vehicle handling performance. The control algorithm is sampled in 10 ms and the vehicle model is sampled in 0.1 ms, which both are recommended by BorgWarner and Lund Formula Student. The reason for the longer sample time for the controller, is because the hardware is expected to be comparably slow and thus, it is not possible and required to update the control algorithm that often as each 0.1 ms.

6

The PI Controller Tuning Process

The process for controller parameter tuning and the different controller parameters are described in this chapter.

6.1 PI Controller for the Nonlinear Model

Using the same PI controller parameters for the different velocities with the nonlinear models, does not give satisfactory result, which can be seen in Figure 6.1a and Figure 6.1b.

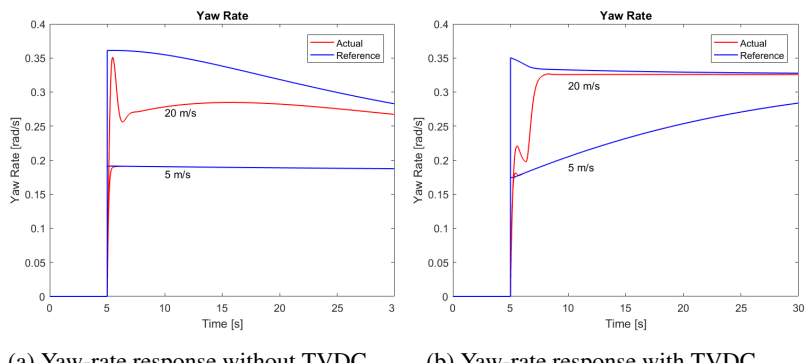


Figure 6.1: Yaw-rate response for velocity 5 m/s and 20 m/s for different PI-tuning parameters.

PI-tuning parameters for velocity 5 m/s are set to $K_p=5$ and $K_i=40$ without having TVDC in the nonlinear model and $K_p=20$ and $K_i=170$ with TVDC included for the nonlinear model. As can be seen in Figures 6.1a and 6.1b, the actual yaw rate

(red) does not follow the desired yaw rate (blue) for velocity 20 m/s with the same PI gains as for velocity 5 m/s in the both models. Thus, different models together with different velocities are given specific PI gains to make the controller more robust, i.e., a gain scheduling is needed. For a constant steering wheel angle, different PI gains are obtained for different velocity intervals [27].

PI Controller for the Linear Model

The PI controller tuning for the linear model is seen in Table 6.1. The controller parameters are independent of the velocity.

Table 6.1: PI controller parameters for all velocities.

K_p	K_i	K_r
800	60	1

PI Controller without TVDC for the Nonlinear Model

The nonlinear model without a TVDC only takes a constant total torque as input. The PI gains can be seen in Table 6.2. K_r is the tracking time constant for anti-windup. The gain scheduling is performed by dividing the velocities into intervals.

Table 6.2: PI controller parameters for different velocities.

Velocity (m/s)	K_p	K_i	K_r
0 - 7	5	40	1
8 - 11	12	150	1
12 - 17	23	270	1
18 - 21	30	300	1

PI Controller with TVDC for the Nonlinear Model

The PI gains can be seen in Table 6.3.

Table 6.3: PI controller parameters for different velocities.

Velocity (m/s)	K_p	K_i	K_r
0 - 9	20	170	1
10 - 12	20	180	1
13 - 17	35	350	1
18 - 21	45	370	1

7

Simulation Results

The results from the simulation for the different models and control strategies are presented and discussed in this chapter.

7.1 Linear Model

The simulation is run for different velocities and with different reference values, which can be seen in the following sections.

Transfer Function

To investigate the linear model, its transfer function is studied. The steering-wheel angle is set to be a disturbance signal into the process and by using MATLAB's own functions, the open-loop transfer function is generated. The transfer function from ΔT to yaw rate (see state-space model in Section 2.3) for velocity 20 m/s, in continuous time is expressed as follows

$$G_{ol}(s) = \frac{0.255s + 766.8}{s^2 + 3001s + 5.161 \cdot 10^6}. \quad (7.1)$$

Using this transfer function, zeros and poles are computed, and the results can be seen in Figure 7.1.

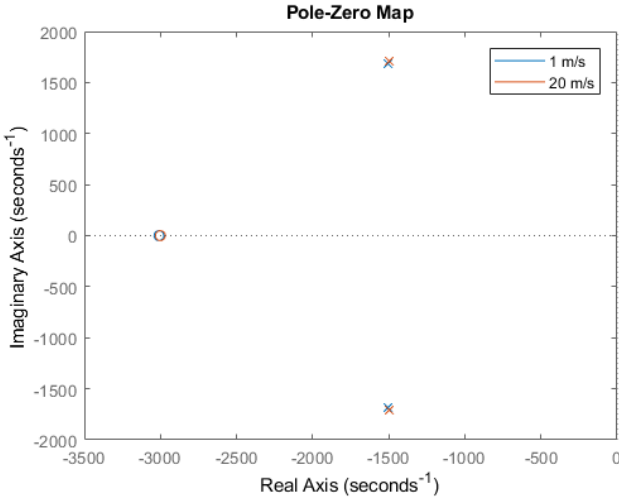


Figure 7.1: Pole placement of the transfer function for the linear single track model. The circle is the zero and the crosses are the poles.

The figure shows the poles and zeros for the velocities 1 m/s and 20 m/s. Since they are basically placed at the same place, it indicates that the linear model will not require different PI tunings for different velocities. This can also be seen in the simulation results in Figure 7.4.

Since the linear single track model is controlled with a PI controller, the closed-loop poles and zeros are also studied to investigate the stability when introducing the controller. The transfer function for the controller used in this case is

$$C(s) = \frac{800s + 60}{s}. \quad (7.2)$$

The closed-loop transfer function is then given by

$$G_{cl}(s) = \frac{G_{ol}(s)C(s)}{1 + G_{ol}(s)C(s)}, \quad (7.3)$$

which for velocity 20 m/s leads to the minimal realization

$$G_{cl}(s) = \frac{204.4s^2 + 6.133 \cdot 10^5 s + 4.6 \cdot 10^4}{s^3 + 3205s^2 + 5.8 \cdot 10^6 s + 4.6 \cdot 10^4}. \quad (7.4)$$

In Figure 7.2, the pole placement is shown for the closed loop.

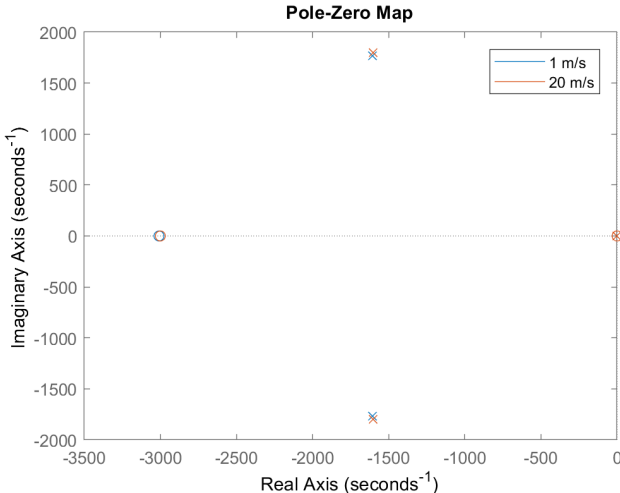


Figure 7.2: Pole placement of the transfer function for the closed loop. The circles are the zeros and the crosses are the poles.

Figure 7.2 shows that the poles and zeros are placed in the left half plane, which indicates stability also for the closed loop.

Simulation 1 The first simulation is based on a constant yaw-rate reference, `YawRateDesired`, and the PI parameters are tuned to give a good control performance for a constant longitudinal velocity, `LongVelocity`. The parameters can be seen in Figure 5.1. The simulation has been done with the constant velocities listed below.

- 1 m/s
- 5 m/s
- 10 m/s
- 15 m/s
- 20 m/s

Figure 7.3 shows the step response for Simulation 1 with the linear single track model, i.e., the PI gains are the same for all velocities, the steering-wheel angle is set to $\pi/3$, and the reference value, i.e., the `YawRateDesired` is set to 0.3 rad/s.

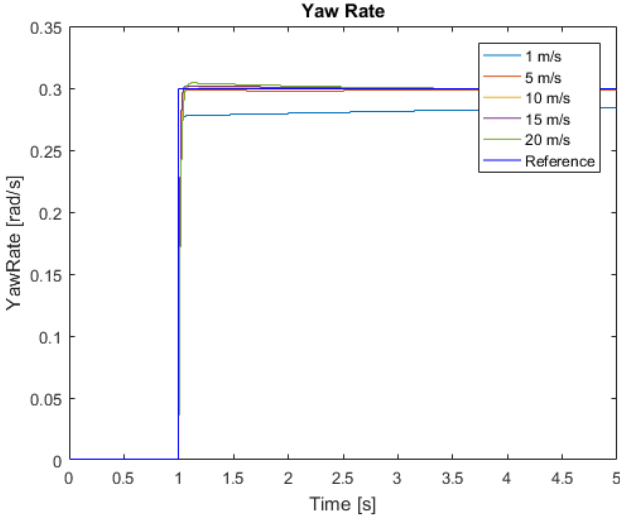


Figure 7.3: Yaw-rate response for different velocities with the same PI controller parameters. The yaw-rate reference does not depend on the driver inputs and is set to 0.3 rad/s.

As seen from the figure, the response values do not differ very much for the different velocities, besides the response for 1 m/s. Observe that this is just one test case. It is clear that different gains are needed for different velocities, which also is in agreement with observations in previous research [19].

Simulation 2 Simulation model 2 contains a block that generates the reference value `YawRateDesired`, which depends on the vehicle's longitudinal velocity, `LongVelocity`, and the drivers steering-wheel angle, `SteeringAngle`. Simulations have been done for the velocities listed below.

- 1 m/s
- 10 m/s
- 20 m/s

This simulation is done to investigate if different controller parameters in different operating regions are needed. Since the vehicle dynamics changes with different velocities, the desired yaw rate will also change. Observe that Simulations 1 and 2 in this section do not take any limitations into consideration.

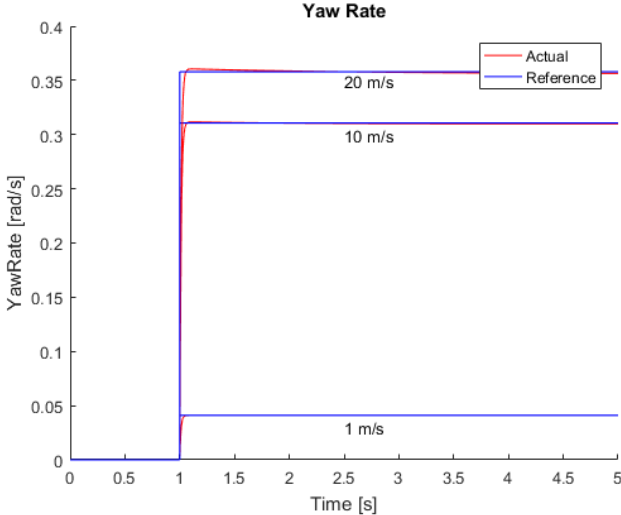


Figure 7.4: Yaw-rate response for different velocities with the same PI-tuned parameters. Yaw-rate reference depends on the driver inputs, where the steering-wheel angle is set to $\pi/3$ rad.

Figure 7.4 shows the vehicle’s yaw rate compared to the yaw-rate reference that is computed with the reference generator when the velocity is 1 m/s, 10 m/s, and 20 m/s. The lowest velocity corresponds to the lowest desired yaw-rate value.

By only studying the single track model, it is clear that a PI controller seems to work well. In this case, it also seems like different PI tunings will not be needed to maintain robust control at different velocities. This result is not fully expected based on Antunes’ work [19] about control gains for different velocities, but probably depends on the linearity of the model.

7.2 Nonlinear Model

Three different driving modes are chosen: lane change, U-turn, and circle, to visualize the effect torque vectoring has during cornering when the vehicle is accelerating. These are presented in a xy-plot, both with actual values given from the vehicle model and values from the reference model to easily see how the vehicle is following desired paths. The different paths are obtained by adding different step responses and implementing global coordinates, which is done as in (2.22) and (2.23). The nonlinear model using TVDC is compared to a nonlinear model with a LSD. This is because the more advanced nonlinear model using a TVDC is a more realistic model than the simpler nonlinear model without a TVDC is, and thus it is comparable with a nonlinear model using LSD.

Nonlinear Model without TVDC

The nonlinear model without TVDC is used to simulate the different driving modes and the corresponding yaw-rate tracking. Two simulations are done and described next.

Simulation 1 The control algorithm is tested with different steering-wheel angles $\pi/9$, $\pi/6$, and $\pi/3$ for a given velocity 10 m/s to verify that the actual yaw-rate value follows the desired yaw rate, independently of what steering-wheel angle that is input to the system. The PI tuning for speed 10 m/s can be seen in Table 6.2.

Figures 7.5, 7.6, and 7.7 show step responses for velocity 10 m/s with different steering-wheel angles. It shows that different steering-wheel angles correspond to different yaw-rate reference values, as expected.

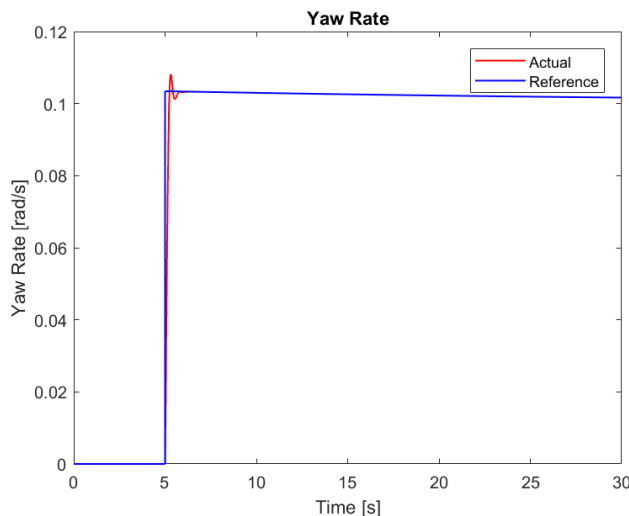


Figure 7.5: Step response for a step steering input at speed 10 m/s and steering-wheel angle of $\pi/9$ rad.

Figure 7.5 shows the yaw-rate response for a steering-wheel angle of $\pi/9$ rad. The actual yaw rate is in red and the desired yaw rate is in blue. It is clear that the controller manages to stabilize the actual yaw rate around the reference value.

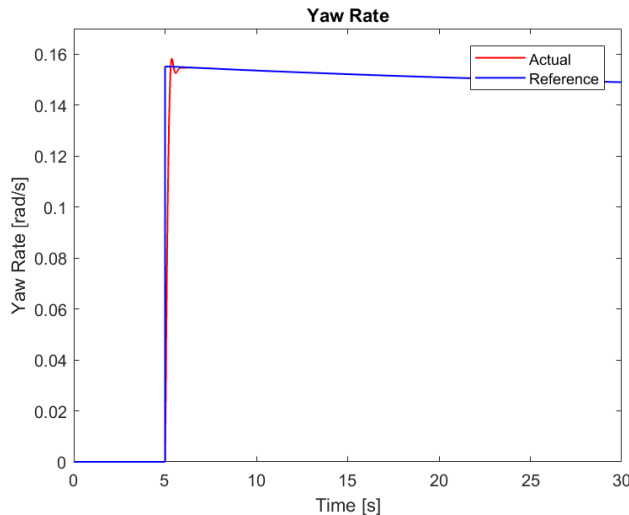


Figure 7.6: Step response for a step steering input at speed 10 m/s and steering-wheel angle of $\pi/6$ rad.

Again it can be observed in Figure 7.6 that the controller is working well.

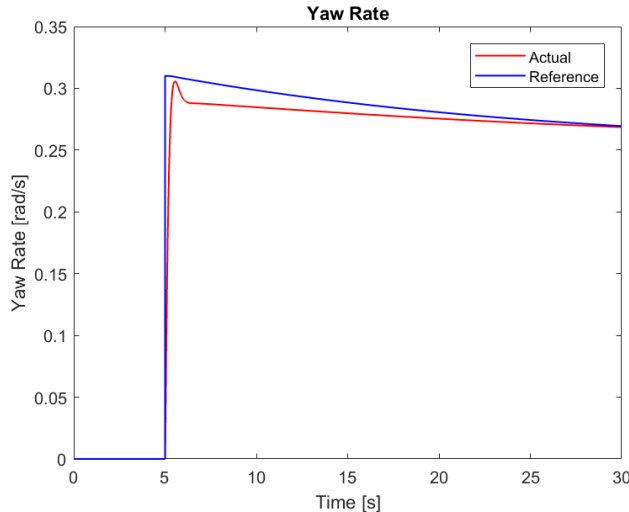


Figure 7.7: Step response for a step steering input at speed 10 m/s and steering-wheel angle of $\pi/3$ rad.

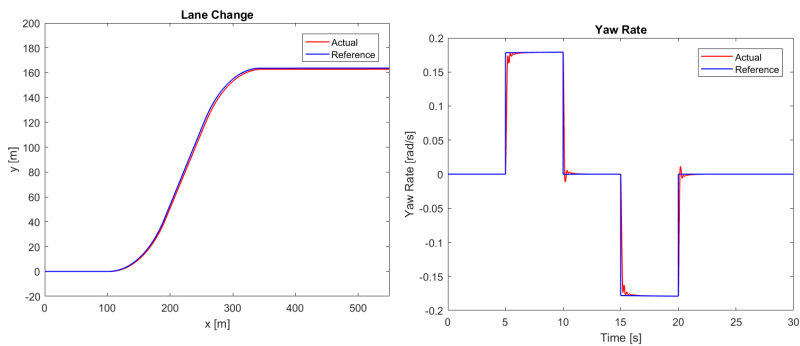
Figure 7.7 shows the yaw-rate response for a steering-wheel angle of $\pi/3$ rad. In this case, the response is not as good as in the two earlier cases. However, this is unavoidable since the torques are in a limited state and can not generate more yaw rate to the vehicle.

Simulation 2 The verification of the algorithm is further tested for the following driving modes:

- lane change,
- U-turn,
- circle.

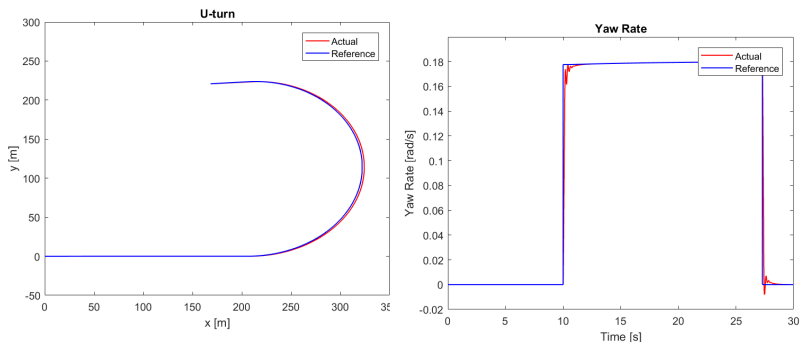
The various cases are based on common driving modes for the Formula Student competitions. The velocities used is 20 m/s because it is the most critical point in motor racing. The goal is to verify that the vehicle trajectory coincides with the desired path for a high speed. The actual yaw rate and the reference value are presented.

The different driving modes and the corresponding yaw-rate tracking for the model without TVDC are seen in Figures 7.8, 7.9, and 7.10.



(a) Vehicle path in a lane change for a step steering input. (b) Yaw-rate tracking of a lane change.

Figure 7.8: Lane change at speed 20 m/s without TVDC.

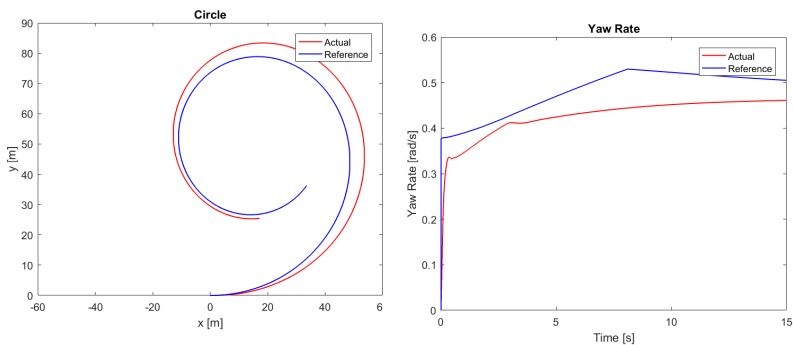


(a) Vehicle path in a U-turn for a step steering input.

(b) Yaw-rate tracking in an U-turn.

Figure 7.9: U-turn at speed 20 m/s without TVDC.

As can be seen in Figures 7.8a and 7.9a, the actual path is perfectly following the reference vehicle trajectory.



(a) Vehicle path in a circle for a step steering input.

(b) Yaw-rate tracking of a circle.

Figure 7.10: Circle at speed 20 m/s without TVDC.

For the circular path, however, the actual path diverges from the reference value as it continues to take a left turn. This is because the torques are in a limited state and the wheels can not generate a better combination of torques.

The yaw rate from the vehicle and the reference model are shown in Figures 7.8b, 7.9b, and 7.10b, and are all compatible with the observed paths.

Nonlinear Model with TVDC

The nonlinear model using TVDC is compared to a nonlinear model with a LSD. Since the FS team has been using 60% locking, the LSD-gain is put to 0.6. When employing the LSD model, the same controller parameters for the gear position and the combustion engine torque were used as for the vehicle model. The control algorithm is tested for different cases. Two simulations are done and described next.

Simulation 1 With the same approach as for the nonlinear model without TVDC, the different driving modes and the corresponding yaw-rate tracking for the model with TVDC is seen in Figures 7.11, 7.12, and 7.13.

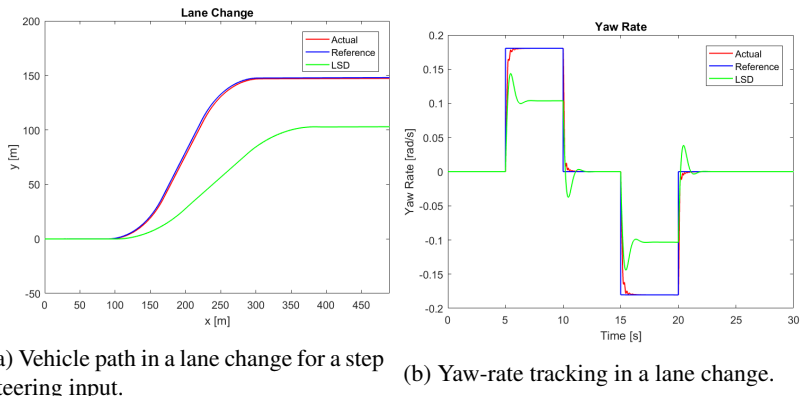
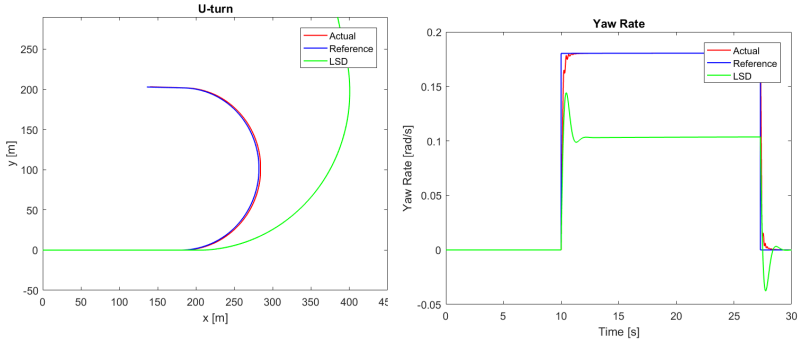


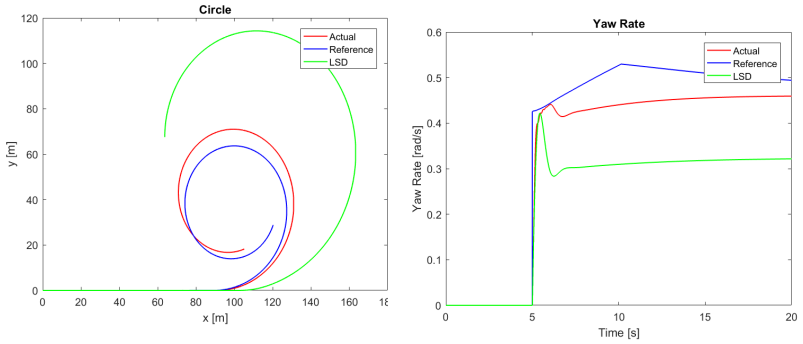
Figure 7.11: Lane change at speed 20 m/s using TVDC.



(a) Vehicle path in a U-turn for a step steering input.

(b) Yaw-rate tracking in an U-turn.

Figure 7.12: U-turn at speed 20 m/s using TVDC.



(a) Vehicle path in a circle for a step steering input.

(b) Yaw-rate tracking in a circle.

Figure 7.13: Circle at speed 20 m/s using TVDC.

The figures show a comparison between a vehicle model using a TVDC (red and blue) and a vehicle model using LSD (green). Again, it is seen that the actual yaw rate is deviating from the desired yaw rate when following circular path and this is due to the limitations of the torques. However, it is clearly seen that the control strategy gives an improved vehicle manuevarblity compared to the LSD.

The yaw rate from the vehicle and the reference model are shown in Figure 7.11b, Figure 7.12b, and Figure 7.13b, and all three are compatible with the observed paths.

Simulation 2 Lastly, the algorithm is tested for an acceleration case with the TVDC. The combustion engine is set to 50 Nm, which ensures an acceleration from the initial value of 10 m/s to 20 m/s. The steering-wheel angle is set to $\pi/2$ rad and hence the critical case of accelerating in a curve is tested.

By studying the yaw-rate response, shown in Figure 7.14, it can be seen that the actual yaw rate using TV is not perfectly following the reference value.

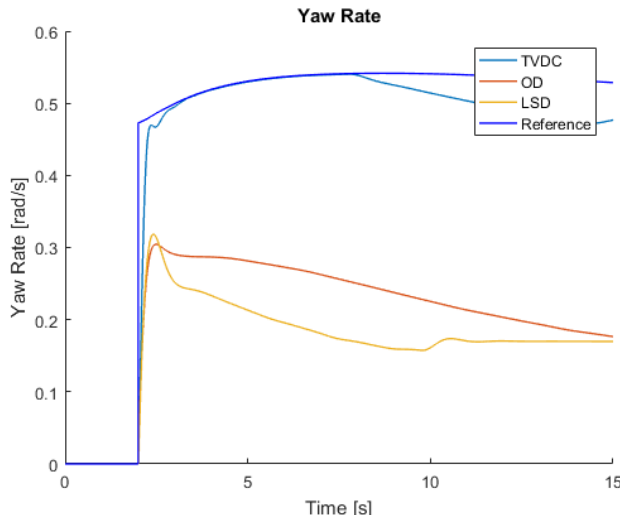


Figure 7.14: Yaw-rate response for an accelerating vehicle with a step steering-wheel input of $\pi/2$ rad.

However, in the torque allocation seen in Figure 7.15, it is clear that the system is saturated by looking at the signal for TVDC left, which has reached its lowest value of 0 Nm. Because of this, it is not physically possible to follow the yaw rate in this case without help from the steering-wheel angle.

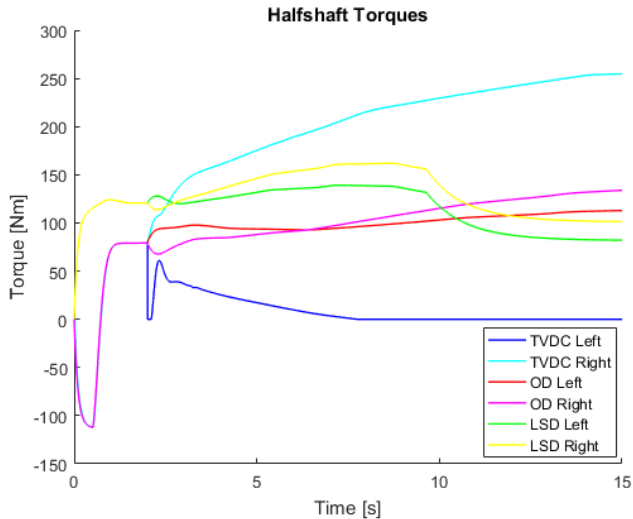


Figure 7.15: Torque on each wheel for different types of differential with a step steering-wheel input of $\pi/2$ rad.

Observe that the three strategies, (TVDC, OD, and LSD) are not completely comparable due to different initial behavior in the models. However, they are good enough to show that TV will be able to improve cornering abilities when comparing with an open differential or limited slip differential.

7.3 Yaw-Rate Error Analysis

An error analysis has been made on the nonlinear model using TVDC. Visual and quantitative results are shown in the following subsections.

Simulation 1

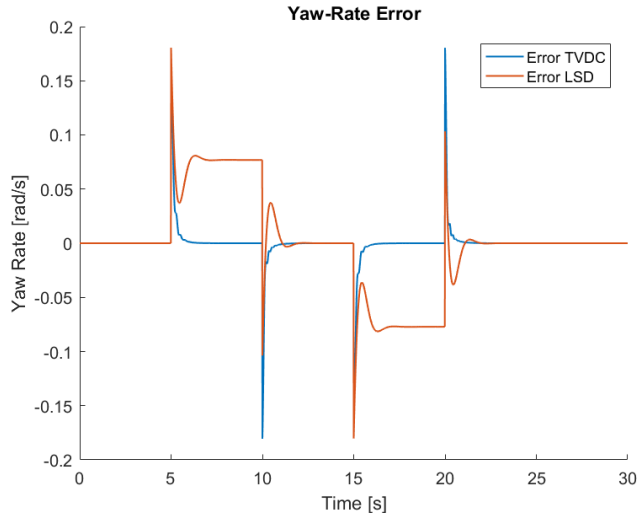


Figure 7.16: Yaw-rate error for a lane change at speed of 20 m/s.

The average absolute yaw-rate error between the desired yaw rate and the actual yaw rate using TVDC is 0.0029 rad/s and the average absolute error using LSD is 0.0271 rad/s in the Figure 7.16.

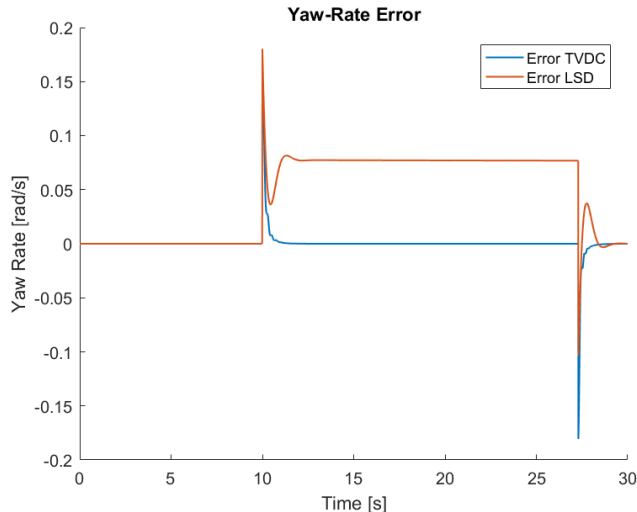


Figure 7.17: Yaw-rate error for a U-turn at speed of 20 m/s.

In Figure 7.17, the average absolute yaw-rate error for a U-turn using a TV is 0.0015 rad/s, which should be compared to the error using an LSD which is 0.0451 rad/s.

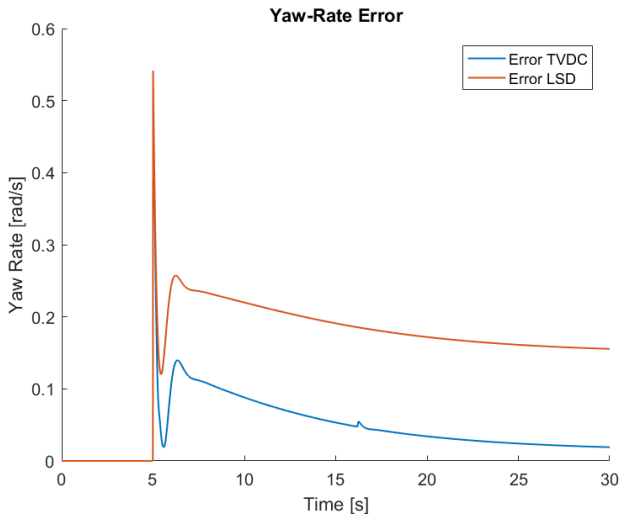


Figure 7.18: Yaw-rate error for a circle at speed of 20 m/s.

In Figure 7.18, the average absolute yaw-rate error for a circular path in speed 20 m/s using a TV is 0.0428 rad/s and for LSD it is 0.1387 rad/s.

Simulation 2 The yaw-rate error for the accelerating case is shown in Figure 7.19.

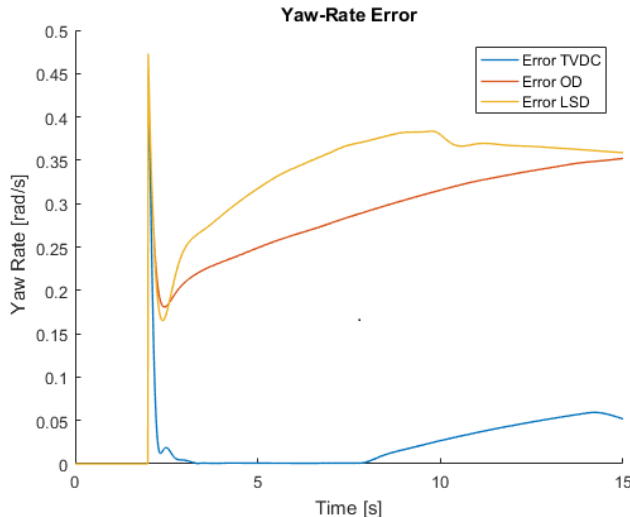


Figure 7.19: Yaw-rate error when the vehicle is accelerating in a curve.

Figure 7.19 shows that TV by far improves the yaw-rate response, which is expected. The average absolute yaw-rate error for TVDC, OD, and LSD is 0.0221 rad/s, 0.2527 rad/s, and 0.2956 rad/s, respectively, in this case.

Summary

The average absolute errors are summarized in Table 7.1.

Table 7.1: Average absolute yaw-rate errors.

	TVDC	LSD	OD
Lane Change	0.0029 rad/s	0.0271 rad/s	-
U-turn	0.0015 rad/s	0.0451 rad/s	-
Circle	0.0428 rad/s	0.1387 rad/s	-
Acceleration	0.0221 rad/s	0.2956 rad/s	0.2527 rad/s

8

Discussion and Conclusions

From the results in section 7 it is clear that a vehicle using a double clutch with a torque-vectoring algorithm can improve a vehicle's performance in terms of cornering but also when accelerating in corners. Also, the more engine torque that is available, i.e., the more torque the driver requests, the better the proposed algorithm is able to help, because the difference in torques on the right and the left wheel can be increased. This leads to the conclusion that a Formula Student Car can benefit of using a torque-vectoring device instead of a LSD as has been used before.

It is hard to make a design criterion considering the step response, since a step change of the steering-wheel angle will never take place. Thus, no exact conclusions can be made about the different step responses besides that the system seems to be stable.

Using the TV algorithm, the rear wheels will be able to take advantage of the fact that the outer wheel has a bigger friction circle and can give the vehicle extra yaw moment. In that way, the control algorithm improves a vehicle's maneuverability when under-steering in curves. However, problems can occur when over-steering. When a vehicle over-steers and the proposed algorithm tries to counteract, it may not have a large enough tire-friction circle on the inner wheel and thus the wheel can start spinning instead.

A drawback with the proposed algorithm is that no consideration has been taken about the fact that the clutches can slip. This will occur when the driver requests torque higher than the upper bound value of the torque limit. The difference in torques will make the clutches to spin, and thus make the clutches warm.

The proposed TV algorithm uses only a PI controller for the feedback loop. The reason to this is because a D-part could create transients which makes the control signal to peak at a certain time. This causes a deviation in the yaw-rate error.

To make the proposed algorithm more complete, the controller can be made more robust by adding more points for the gain scheduling. Another way to make the gain scheduling more complex is to add another gain-scheduling variable. In this

case, the longitudinal velocity was used as a control parameter but the combustion engine torque could also be used since the driver can demand higher torques on the wheels that differ from those given in this report. What concerns gain scheduling, the performances and sometimes stability is only guaranteed at the specific design points or intervals.

As can be seen in Table 7.1, the average yaw-rate error using torque vectoring is one hundredth lower than using the limited slip differential. It is noticeable that for the circular path, the average yaw-rate error is higher than for a lane change or a U-turn. However, the results show that the TV approach improves the vehicle maneuver and performance.

When it comes to safety, the algorithm could be a solution to avoid for example under-steering. At the same time, it can give an unnatural feeling to the driver, which in turn can make the driver react in a way that would result in a bad vehicle maneuver. Therefore, when developing this type of algorithm, it is important to have in mind that the driver should have good experience and knowledge, and should be ready to handle this type of vehicle. Another possibility is to make sure that the control structure will not cause unnatural feeling to the driver. An alternative way to construct the control algorithm is to add a feedforward loop without a PI controller. The algorithm would then instead only control what the driver demands and not the error. Another solution to avoid unnatural driver feeling could be to investigate other ways to estimate the desired yaw rate, which plays a big role in the controller implemented in this thesis. To improve the accuracy of the algorithm, the longitudinal velocity and vertical tire loads could also be estimated in other ways. They will, even so, not affect the unnatural feeling. It is also possible to combine feedforward and feedback controller, which would give a more robust control.

Since the proposed algorithm has not been able to be tested on a test-rig, the authors of this report cannot say if the control algorithm can be applied generally. However, the final validation will be made with a Formula Student car developed for competition in summer 2020, although the actual control algorithm will not be used until the competition in summer 2021.

For future research, one could implement an algorithm that enables individual brake control to the wheels. This implicates a decrease in moment on one and increase on the second driving wheel. Another aspect to further investigate is the mapping from the steering-wheel angle to road wheel angle and to use compatible cornering stiffnesses provided by Lund Formula Student itself. In that way, the vehicle model would be identical to a Formula Student car. If a signal is missing or deviates much from the nominal value, it would be necessary to implement an error handling strategy.

This algorithm is implemented with one type of tires taken into account and thus, no consideration has been made about other types of tires. For future research, other tires that do not have the same characteristics as the ones modeled in this project might need other PI controller gains.

Bibliography

- [1] Euro NCAP - For Safer Cars, Electronic Stability Control, available: <https://www.euroncap.com/sv/fordonssaekerhet/foerklaring-av-betygen/foerarstoeedsystem/electronic-stability-control/> [2019-01-28]
- [2] S. Kalkan, *Twin clutch with torque vectoring capabilities for Formula Student vehicle*. Goal Document from M.Sc. Thesis. Department of Mechanical Engineering, Lund University, Lund, Sweden, 2018.
- [3] E. Siampis, E. Velenis & S. Longo, *Rear wheel torque vectoring model predictive control with velocity regulation for electric vehicles*. Vehicle System Dynamics, 53:11, 2015, p. 1555-1579, DOI: 10.1080/00423114.2015.1064972
- [4] S. Kalkan, *A final drive device for torque vectoring in small race cars*, M.Sc. Thesis, Department of Mechanical Engineering, Lund University, Lund, Sweden, 2019, ISSN: 0282-1990.
- [5] *Lund Formula Student*, available: <http://www.formulastudent.lu.se/formula-student/> [2019-04-02]
- [6] Lund Formula Student, Powerpoint presentation by Lund Formula Student, *Lund Formula Student goes Electric*, Lund University, Lund, Sweden.
- [7] W. Berg, e-mail correspondence with Madeleine Rosicki, 2019, Landskrona, Sweden.
- [8] R. Rajamani, *Vehicle dynamics and control*. Springer Science & Business Media, New York, USA, 2011.
- [9] J. A. Barlage, T. Brink, H. Cabral, D. Herven, V. P. Jones, J. Maguire, T. L. Perttola, J. A. Peterson, L. Pritchard, *All-Wheel Drive - A Practical Manual*, second edition, Landskrona, BorgWarner Inc., 2016, p. 47-71.
- [10] D. Blom, employee at BorgWarner, discussion with Mia Grahovic and Madeleine Rosicki, BorgWarner, 2019, Landskrona, Sweden.

Bibliography

- [11] R. P. Osborn, T. Shim, *Independent Control of All-Wheel-Drive Torque Distribution*. SAE International, SAE Technical Paper Series, 2004. DOI: 10.4271/2004-01-2052
- [12] K. Sawase, Y. Ushiroda, K. Inoue, *Effect of the Right-and-left Torque Vectoring System in Various Types of Drivetrain*, SAE International, SAE Technical Paper Series, 2007, DOI: 10.4271/2007-01-3645
- [13] E. N. Smith, E. Velenis, D. Tavernini & D. Cao, *Effect of handling characteristics on minimum time cornering with torque vectoring*. Vehicle System Dynamics, 56:2, 2018, p. 221-248, DOI: 10.1080/00423114.2017.1371771
- [14] EMRAX Innovative Motors, EMRAX 228, available: <https://emrax.com/products/emrax-228/> [2019-04-04]
- [15] Digi-Key Electronics, ZF Electronics GS100701, available: <https://www.digikey.se/products/en?keywords=GS100701> [2019-04-04]
- [16] Gill, GS Position 1498 - Blade 360 Rotary Non-Contact Position Sensor, available: <https://www.gillsc.com/assets/Uploads/GSposition-PD1498-Iss-5.pdf> [2019-04-04]
- [17] MathWorks, *Simulink*, available: <https://se.mathworks.com/products/simulink.html> [2019-05-10]
- [18] J. Öhr, *Anti-windup and control of systems with multiple input saturations. Tools, solutions and case studies*, Ph.D Thesis, Department of Signals and Systems, Uppsala University, Uppsala, Sweden, 2003, p. 1-214, ISBN 91-506-1691-9.
- [19] J. P. M. Antunes, *Torque Vectoring for a Formula Student Prototype.*, M.Sc. Thesis, Department of Mechanical Engineering, Lisboa University, 2017, p. 1-77.
- [20] E. Mikulas, M. Gulán & G. Takács, *Model Predictive Torque Vectoring Control for a Formula Student Electric Racing Car*, European Control Conference (ECC), 2018, p. 581-588, DOI: 10.23919/ECC.2018.8550124.
- [21] A. Stoop, *Design and Implementation of Torque Vectoring for the Forze Racing Car*, M.Sc. Thesis, Department of Mechanical Engineering, Delft Center for Systems and Control, Delft University of Technology, Delft, The Netherlands, 2014, p. 1-82.
- [22] J. Gerhard, M-C. Laiou, M. Mönningmann, W. Marquardt, M. Lakehal-Ayat, E. Adeke, R. Busch, *Robust yaw control design with active differential and active roll control systems*, Elsevier IFAC Publications, 2004, p. 73-78.
- [23] E. Siampis, M. Massaro, E. Velenis, *Electric rear axle torque vectoring for combined yaw stability and velocity control near the limit of handling*, 52nd IEEE Conference on Decision and Control (CDC), Florence, Italy, October 10-13, 2013, p. 1552-1557. DOI: 10.1109/CDC.2013.6760103.

- [24] E. Wennerström, *Fordonsteknik*, compendium, 7:th edition, Department of Vehicle Dynamics, Kungliga tekniska högskolan, Stockholm, 1996, chapter 2.3 p. 2.15.
- [25] M. Canale, L. Fagiano, M. Milanese, P. Borodani, *Robust vehicle yaw control using an active differential and IMC techniques*, Control Engineering Practice, 15(8), 2007, p. 923–941. DOI: 10.1016/j.conengprac.2006.11.012.
- [26] Q. Lie, G. Kasier, S. Boonto, H. Werner, F. Holzmann, B. Chretien, M. Koerste, *Two-degree-of-freedom LPV control for a through-the-road hybrid electric vehicle via torque vectoring*, IEEE Conference on Decision and Control and European Control Conference (CDC-ECC), Orlando, FL, USA, December 12–15, 2011, p. 1274. DOI: 10.1109/CDC.2011.6161175.
- [27] G. J. L. Naus, *Gain scheduling - robust design and automated tuning of automotive controllers*, Department of Advanced Chassis and Transport Systems, Eindhoven University of Technology, Eindhoven, The Netherlands, Report number 106, 2009, p. 3-4.

Lund University Department of Automatic Control Box 118 SE-221 00 Lund Sweden		<i>Document name</i> MASTER'S THESIS
		<i>Date of issue</i> June 2019
		<i>Document Number</i> TFRT- 6081
<i>Author(s)</i> Mia Grahovic Madeleine Rosicki		<i>Supervisor</i> Mariann Kempe, BorgWarner Anders Robertsson, Dept. of Automatic Control, Lund University, Sweden Anders Rantzer, Dept. of Automatic Control, Lund University, Sweden (examiner)
<i>Title and subtitle</i> Development and Evaluation of a Torque-Vectoring Algorithm on RWD Racing Cars using a Dual Clutch		
<i>Abstract</i> <p>Vehicle safety and vehicle performance are becoming more and more important for the society and many students, doctoral students, and researchers are interested in this field. Formula Student is a student competition that enables students to develop their own racing vehicles without any strict rules on how the vehicle should be controlled. The competition rules are instead directed into vehicle design and maneuverability on the track. This thesis was performed in collaboration with Lund Formula Student and BorgWarner. It presents a torque-vectoring algorithm that is planned to be implemented on a Formula Student car for next years competition in 2021. The Formula Student car will use a double clutch that is also developed at BorgWarner by a student in Mechanical Engineering at Lund University. The double clutch enables independent control of torques for each rear wheel.</p> <p>The algorithm was developed in MATLAB/Simulink, mainly using vehicle models provided by BorgWarner. The goal with the torque-vectoring algorithm is to improve the vehicle's accelerating behavior while cornering.</p> <p>The nonlinear model that uses a torque-vectoring dual clutch (TVDC) is compared to another nonlinear vehicle model that represents a Formula Student vehicle using a limited slip differential (LSD) clutch. The controller is using yaw rate as a control signal. The results show that the vehicle trajectories for a lane change and U-turn coincide with the reference value, for the circular path, whereas the actual yaw rate value diverges from the reference value after some time. Overall, the vehicle can better follow the desired path with the proposed torque-vectoring algorithm for a double clutch than a vehicle using an LSD clutch. When the vehicle is accelerating, it is clearly seen that for the TVDC, the actual yaw rate is following the desired yaw rate better than using open differential (OD) or LSD. Considering the yaw-rate error analysis, it is clearly seen that the error is smaller for a lane change and a U-turn than it is when the vehicle is following a circular path. Overall, the yaw-rate error is smaller when employing TVDC than without.</p>		
<i>Keywords</i>		
<i>Classification system and/or index terms (if any)</i>		
<i>Supplementary bibliographical information</i>		
<i>ISSN and key title</i> 0280-5316		<i>ISBN</i>
<i>Language</i> English	<i>Number of pages</i> 1-67	<i>Recipient's notes</i>
<i>Security classification</i>		